Clays and Clay Minerals, Vol. 59, No. 4, 359–377, 2011.

EVIDENCE FOR LOW-GRADE METAMORPHISM, HYDROTHERMAL ALTERATION, AND DIAGENESIS ON MARS FROM PHYLLOSILICATE MINERAL ASSEMBLAGES

Bethany L. Ehlmann[1,2,*,†], John F. Mustard[2], Roger N. Clark[3], Gregg A. Swayze[3], and Scott L. Murchie[4]

[1] Institut d'Astrophysique Spatiale, Université Paris-Sud 11, Orsay, 91405, France
[2] Department of Geological Sciences, Brown University, Providence, Rhode Island, 02912 USA
[3] US Geological Survey, Denver, Colorado, 80225 USA
[4] Johns Hopkins University Applied Physics Laboratory, Laurel, Maryland, 20723 USA

Abstract—The enhanced spatial and spectral resolution provided by the Compact Reconnaissance Imaging Spectrometer for Mars (CRISM) on the Mars Reconnaissance Orbiter (MRO) has led to the discovery of numerous hydrated silicate minerals on Mars, particularly in the ancient, cratered crust comprising the southern highlands. Phases recently identified using visible/near-infrared spectra include: smectite, chlorite, prehnite, high-charge phyllosilicates (illite or muscovite), the zeolite analcime, opaline silica, and serpentine. Some mineral assemblages represent the products of aqueous alteration at elevated temperatures. Geologic occurrences of these mineral assemblages are described using examples from west of the Isidis basin near the Nili Fossae and with reference to differences in implied temperature, fluid composition, and starting materials during alteration. The alteration minerals are not distributed homogeneously. Rather, certain craters host distinctive alteration assemblages: (1) prehnite-chlorite-silica, (2) analcime-silica-Fe,Mg-smectite-chlorite, (3) chlorite-illite (muscovite), and (4) serpentine, which furthermore has been found in bedrock units. These assemblages contrast with the prevalence of solely Fe,Mg-smectites in most phyllosilicate-bearing terrains on Mars, and they represent materials altered at depth then exposed by cratering. Of the minerals found to date, prehnite provides the clearest evidence for subsurface, hydrothermal/metamorphic alteration, as it forms only under highly restricted conditions (T = 200−400ºC). Multiple mechanisms exist for forming the other individual minerals; however, the most likely formation mechanisms for the characteristic mineralogic assemblages observed are, for (1) and (2), low-grade metamorphism or hydrothermal (<400ºC) circulation of fluids in basalt; for (3), transformation of trioctahedral smectites to chlorite and dioctahedral smectites to illite during diagenesis; and for (4), low-grade metamorphism or hydrothermal (<400ºC) circulation of fluids in ultramafic rocks. Evidence for high-grade metamorphism at elevated pressures or temperatures >400ºC has not been found.

Key Words—Analcime, Chlorite, Craters, Diagenesis, Hydrothermal Alteration, Illite, Infrared Spectroscopy, Mars, Metamorphism, Muscovite, Phyllosilicates, Prehnite, Serpentine, Silica, Zeolites.

INTRODUCTION

High spatial and spectral resolution orbital visible/near-infrared (VNIR) spectroscopy of Mars has greatly expanded capabilities for the detection of alteration mineral phases and examination of their geologic context. The *Observatoire pour la Minéralogie, l'Eau, les Glaces, et l'Activité* (OMEGA) on Mars Express has acquired near global coverage at hundreds of meters per pixel resolution and revealed deposits of phyllosilicates, which are mostly smectite clays, as well as sulfates (Bibring *et al.*, 2005; Poulet *et al.*, 2005; Gendrin *et al.*, 2005). Data from the Compact Reconnaissance Imaging Spectrometer for Mars (CRISM) onboard the Mars Reconnaissance Orbiter (MRO) have subsequently revealed additional diversity in alteration mineral phases including carbonates, zeolites, additional sulfates, and additional hydrated silicates, such as kaolinite, chlorite, serpentine, illite (or muscovite), and opaline silica (Mustard *et al.*, 2008; Milliken *et al.*, 2008; Bishop *et al.*, 2008; Ehlmann *et al.*, 2008, 2009).

The presence of these alteration minerals is interesting in its own right as an indication of past chemical reactions of water with Mars' basaltic rocks and sediments. In some instances, further information about the precise geochemical conditions of aqueous alteration (temperature, pressure, pH, Eh, and ion activities) may be gained by considering the minerals, their assemblages, and their geologic context in conjunction with knowledge about the thermodynamic and kinetic limitations on mineral formation, derived from terrestrial experience. OMEGA found that phyllosilicates were restricted to Mars' oldest Noachian terrains (>3.7 Gy) while sulfates were found in younger Hesperian terrains (~2.9−3.7 Gy). This suggested a directional evolution in Mars' geologic history whereby initially neutral to

* E-mail address of corresponding author:
ehlmann@gps.caltech.edu
† Present address: Division of Geological and Planetary Sciences, California Institute of Technology, MC170-25 Pasadena, California, 91125, USA
DOI: 10.1346/CCMN.2011.0590402

alkaline conditions, under which long-term, water-rock interactions were needed to form Fe,Mg-smectites, were replaced by ephemerally wet, more acidic environments where precipitation of sulfate evaporites dominated (Bibring *et al.*, 2006). The CRISM findings have largely supported this paradigm but have also permitted the discrimination of at least 11 distinct alteration environments on the basis of morphology and mineral assemblage (Murchie *et al.*, 2009a). The present study focused was on a subset of alteration minerals recently identified by CRISM, which suggests that in Mars' past some aqueous alteration took place at elevated temperatures. Evidence is reviewed that localized hydrothermal, low-grade metamorphic, or diagenetic activity were some of the processes forming and modifying hydrated silicate minerals on Noachian Mars.

Ancient Mars (>3 Gy) possessed both surface (Fassett and Head, 2008) and subsurface (Andrews-Hanna *et al.*, 2007) waters. Sources of heat were available from impact cratering, volcanism, and a planetary geothermal gradient higher than present (*e.g.* Parmentier and Zuber, 2007). Hence, numerous authors have predicted hydrothermal or metamorphic alteration of the Martian crust by water-rock interactions. Evidence includes trace quantities of primary hydrous minerals, in particular amphiboles and micas, in the so-called SNC (shergottite, nahklite, chassigny) classes of meteorites (Gooding *et al.*, 1992); carbonate isotopic values in ALH84001 (Harvey and McSween, 1996); and enriched D/H ratios in the Martian crust and atmosphere (Jakosky and Jones, 1994). The occurrence and mineralogy of hydrothermal systems depend on water availability, the composition of the host rocks, and the temperature and composition of circulating fluids. Based on experience with terrestrial systems, the existence of phyllosilicates, zeolites, carbonates, and sulfates has been predicted in hydrothermal systems generated in Mars' basaltic rocks following impacts (Newsom, 1980; Allen *et al.*, 1982). Models have shown that, given sufficient water in the regolith, impact-induced hydrothermal systems could last up to tens of thousands of years in the subsurface beneath craters (Rathbun and Squyres, 2002; Abramov and Kring, 2005; Barnhart *et al.*, 2010) producing zoned phyllosilicate-bearing mineral assemblages (Schwenzer and Kring, 2009). Hydrothermal activity has also been invoked to explain some apparently water-related features around volcanoes such as incised valleys on Martian stratovolcano slopes (Gulick and Baker, 1990; Farmer, 1996, and references therein). The expected mineralogic assemblages resulting from hydrothermal circulation beneath lava flows have been calculated (Griffith and Shock, 1997). Some crustal cooling models indicate that hydrothermal activity in the upper 10 km of crust may have played a substantial role in heat loss on early Mars (Parmentier and Zuber, 2007). Finally, one possible explanation for the existence of methane in the present-day Martian atmosphere is its release as a product of ongoing serpentinization, the reaction of ultramafic rocks and water at elevated temperatures (Mumma *et al.*, 2009).

Below, methodology is described for delineating indicator minerals for metamorphism, hydrothermal activity, and diagenesis and then detecting them remotely from Mars orbit. Examples are given of the geologic settings of four diagnostic minerals or mineral assemblages, which indicate alteration at elevated temperatures: (1) prehnite-chlorite-silica, (2) analcime-silica-chlorite-Fe,Mg-smectite, (3) chlorite-illite (muscovite), and (4) serpentine. The past temperature, pressure, and geochemical conditions indicated are discussed. Finally, some suggestions are made for future research and the potential of these types of sites as targets for future surface exploration.

METHODS

Delineating diagnostic minerals

A metamorphic facies is "a set of metamorphic mineral assemblages...showing a regular relationship between mineral composition and bulk chemical composition, such that different metamorphic facies...appear to be related to different metamorphic conditions, in particular temperature (T) and pressure (P), although other variables such as P_{H_2O} may also be important." (Smulikowski *et al.*, 2003). The facies have a characteristic distribution as a function of temperature and pressure (Figure 1), though the composition of interacting fluids and kinetic effects also dictate the precise mineralogy. The interpretations of mineralogy herein are based on mafic or ultramafic protoliths, an assumption justified by orbital and landed examination of the composition of Mars' crust (Hoefen *et al.*, 2003; Rogers and Christensen, 2007; McSween *et al.*, 2009). Hence, for facies recognition, typical mineral assemblages from basaltic protoliths (Table 1) are most relevant.

For any given facies, minerals of metamorphosed terrains may be divided into common, diagnostic, and forbidden (Chen *et al.*, 1983 after Zwart *et al.*, 1967). Common minerals are those typically found within a facies. Diagnostic minerals specifically indicate particular P, T values during alteration *via* thermodynamic restrictions on the conditions in which they form. Assemblages of diagnostic + common minerals provide a routine field and petrologic means of identifying metamorphic facies and thus particular P,T conditions experienced by the rock. Forbidden minerals are those which do not belong in a particular metamorphic facies because they definitively indicate particular P,T conditions of another facies.

For relatively low-temperature alteration, which, as discussed below, is most relevant to the mineral phases discovered on Mars to date, boundaries between sub-greenschist-facies metamorphism, zeolite-facies

https://doi.org/10.1346/CCMN.2011.0590402 Published online by Cambridge University Press

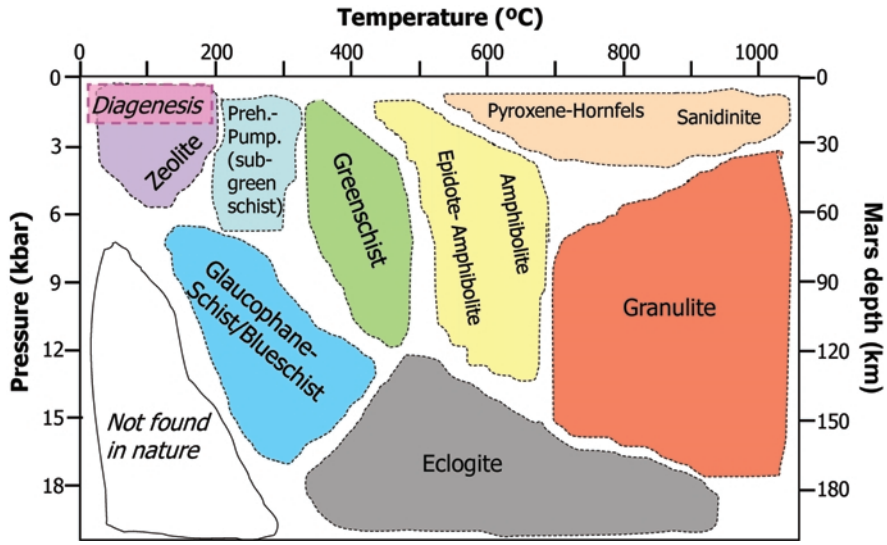

Figure 1. Pressure-temperature metamorphic-facies diagram after Spear (1995). Greater depths than on Earth are required to achieve a given pressure because of Mars' lower gravity. Preh. = prehnite; Pump. = pumpellyite.

metamorphism, hydrothermalism, and diagenesis are poorly defined, with different authors adopting different conventions through time (see Arkai *et al.*, 2003 for a review). Sub-greenschist metamorphism occurs at temperatures of <~300–400ºC and pressures typically <4 kbar but extending to 8 kbar (Schiffman and Day, 1999). The sub-greenschist facies is defined by the thermodynamic stability and presence of pumpellyite and prehnite.

The lowest metamorphic temperature and pressure conditions are represented by the zeolite facies. Zeolites are attributed to alteration at low temperatures in the presence of CO_2-poor or non-CO_2 bearing alkaline fluids (*e.g.* Hay, 1986). Zeolites bridge the gap between

Table 1. Common diagenetic mineral assemblages and diagnostic and common minerals for select metamorphic facies for a basaltic protolith (see Spear, 1995, chapter 11 for an overview, and specific references below).

P-T assemblage/facies	Diagnostic minerals and assemblages	Common minerals and assemblages	Specific references
Diagenesis	chlorite, illite or muscovite, and mixed-layer clays (chlorite/smectite, illite-smectite); celadonite+Fe,Mg-smectite		Cann (1979); Meunier (2005)
Zeolite	zeolite minerals	Heulandite + analcime + quartz, laumontite, stilbite, wairakite	Arkai *et al.* (2003); Coombs *et al.* (1959)
Sub-greenschist (prehnite-pumpellyite)	prehnite, pumpellyite	Prehnite + pumpellyite + chlorite, prehnite + chlorite + quartz, epidote + calcite + quartz + chlorite	Frey and Robinson (1999)
Greenschist	actinolite, cummingtonite	Chlorite + albite + actinolite (cummingtonite) + epidote + zoisite + quartz	Smulikowski *et al.* (2003); Philpotts and Ague (2009)
Amphibolite	hornblende	Hornblende + albite + epidote + chlorite, hornblende + Ca plagioclase (+ quartz + garnet)	Smulikowski *et al.* (2007); Philpotts and Ague (2009)
Blueschist	glaucophane, lawsonite	Glaucophane + lawsonite + garnet + quartz, glaucophane + lawsonite, glaucophane + lawsonite + jadeite	Smulikowski *et al.* (2007); Philpotts and Ague (2009)

https://doi.org/10.1346/CCMN.2011.0590402 Published online by Cambridge University Press

diagenetic and metamorphic conditions. In the past, some authors divided the facies into a diagenetic field, which included heulandite or analcime (plus quartz), and a metamorphic field, which included laumontite. However, the zeolite facies is now regarded as a single metamorphic facies regardless of the origin of the indicator minerals (Arkai *et al.*, 2003). The upper temperature stability of the zeolite facies is ~300ºC with the precise mineral assemblage dependent on P, P_{H_2O}, and the activities of K, Na, Ca, and Si in solution (Coombs *et al.*, 1959). Commonly, zeolite-facies minerals form only locally. Complete chemical equilibrium is not achieved for the entire rock because of the low temperatures of metamorphism. Furthermore, unmetamorphosed basalt is nearly anhydrous, and H_2O must be added to the rock to produce low-grade metamorphic assemblages. The rock must be sufficiently permeable to fluid entry and, therefore, zeolites are typically only found in fractures, vugs, and other cavities. Numerous types of zeolites are found and have been used in conjunction with thermodynamic data to determine temperatures of alteration in terrestrial hydrothermal environments (*e.g.* Weisenberger and Selbekk, 2008).

Finally, during the thermal- and pressure-related maturation of sediments, *i.e.* diagenesis, smectites reorder into other hydrous phases (*e.g.* Środoń, 1999; Meunier, 2005). The degree of transformation depends on time and temperature when sufficient water is available to promote transformations (*e.g.* Whitney, 1990). Provided that sufficient K^+ is available in fluids, dioctahedral smectites such as montmorillonite convert to mixed-layer illite-smectite clays, then to illite, then to micas such as muscovite with more advanced diagenesis at higher temperatures (*e.g.* Hower *et al.*, 1976; Yau *et al.*, 1988; Fleet and Howie, 2006). Provided that sufficient Mg^{2+} is available, trioctahedral smectites such as saponite transform to corrensite (a 1:1 mixed-layer chlorite-smectite) then to chlorite with increasing grade (Merriman and Peacor, 1999, and references therein).

Using infrared spectroscopy to identify diagnostic minerals/assemblages

Visible/near-infrared reflectance spectroscopy over the 0.4−2.5 μm wavelength range permits the detection and differentiation of numerous minerals (*e.g.* Clark *et al.*, 1990) and has been used extensively in the characterization of phyllosilicates, carbonates, and zeolites (*e.g.* Gaffey, 1987; Bishop *et al.*, 2002a, 2002b; Cloutis *et al.*, 2002). Broad electronic absorptions, resulting from charge transfer and ligand-field transitions, indicate the presence of transition metals, most commonly Fe, in the mineral structure while sharper combination and overtone vibrational absorptions indicate the presence of H_2O, metal-OH, and CO_3 in minerals.

The shape and position of several diagnostic absorption bands are used to identify a given mineral. The presence of H_2O in the mineral structure is expressed near 1.9 μm by a combination tone of the fundamental bending and stretching vibrations of the water molecule (Hunt and Salisbury, 1970). An overtone of the metal-OH stretching vibration occurs near 1.4 μm, as does an H_2O combination tone (*e.g.* Bishop *et al.*, 1994). From 2.1 to 2.5 μm, additional structural metal-OH combination stretching plus bending vibrations are found, and their precise wavelength position depends on the type of cation and mineral structure. For example, Fe-OH absorptions due to octahedral cations in smectite clays are found near 2.28 μm whereas Al-OH absorptions are found near 2.20 μm. The position of the OH overtone near 1.4 μm also shifts depending on composition (*e.g.* Clark *et al.*, 1990; Bishop *et al.*, 2002a, 2002b). Overtones and combinations of fundamental vibrations related to H_2O in zeolites (Cloutis *et al.*, 2002) and CO_3 in carbonates (Gaffey, 1987) are also diagnostic and found in the 2−2.6 μm wavelength region.

Not all minerals produce diagnostic spectral signatures in the VNIR wavelength range, however. For example, of the minerals comprising metamorphic facies in Table 1, quartz and feldspars do not possess identifiable features in this spectral region (an exception is when these phases are hydrated as in opaline silica or contain substantial Fe impurities as in lunar Fe-bearing plagioclases). Typically, in natural rocks and sediments, only 1 or 2 phases may be apparent in a single spectrum even though the area sampled may consist of more than two minerals. When mixed areally ('checkerboard mixing'), minerals contribute linearly to the spectrum; however, in semi-transparent or fine-grained samples, 'intimate mixing' dominates instead as light interacts with grains of multiple compositions. This is typically the case for remote sensing applications and, hence, minerals comprising surface rocks and sediments contribute non-linearly to observed spectral properties, out of proportion to their abundance (Clark, 1999). In synthethic mixtures measured in the laboratory, phases can typically be detected at the 10% level (or less), but in natural samples the threshold can be higher (*e.g.* Ehlmann *et al.*, 2010a). The reasons are not understood completely although the optical properties of some minerals make them spectrally dominant, and rock texture may play a role in detectability. Nevertheless, keeping these limitations in mind, the mineralogic assemblage characteristic of a particular lithologic unit or group of units can sometimes be determined and used to infer environmental conditions by considering those minerals that are detected by VNIR while bearing in mind the potential reasons for non-detection of other minerals.

Fortunately, several metamorphic minerals, the presence of which is diagnostic of particular facies, have distinctive near-infrared spectroscopic signatures (Figure 2). Some zeolite-facies minerals can be clearly distinguished from other phases by relatively deep

https://doi.org/10.1346/CCMN.2011.0590402 Published online by Cambridge University Press

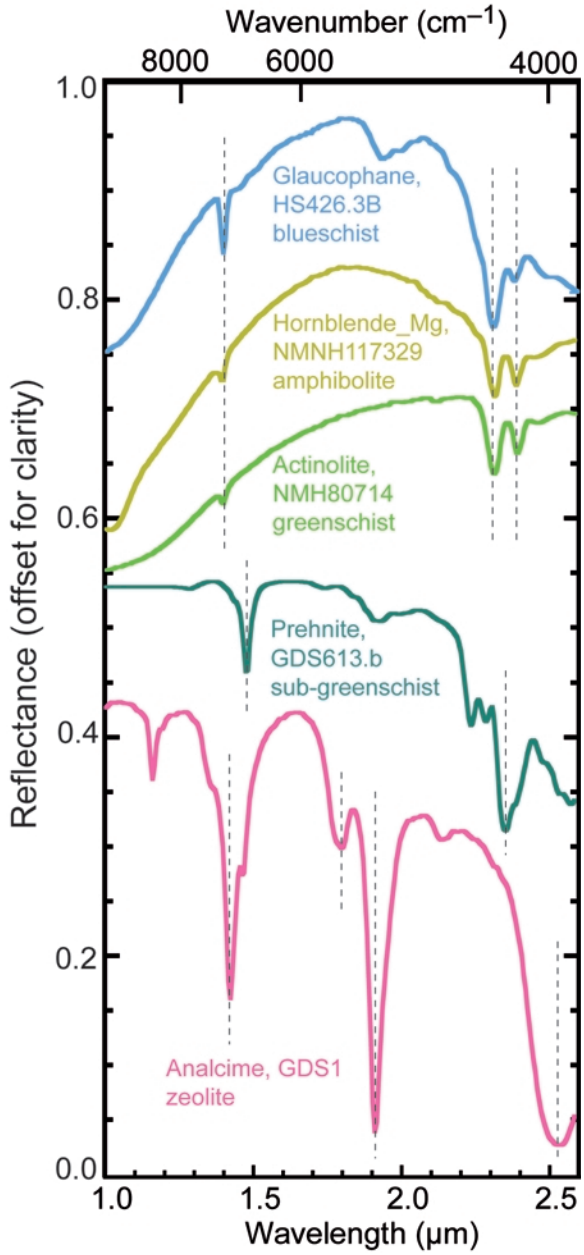

Figure 2. Sample VNIR spectra of diagnostic metamorphic minerals acquired in a laboratory (Clark *et al.*, 2007). Distinctive shapes and positions of absorption features permit these minerals to be identified on the surface of Mars using CRISM spectral data in the 1.0–2.6 μm wavelength range.

water-related absorption features (*e.g.* at 1.16, 1.42, 1.79, 1.91, 2.13, and 2.52 μm in analcime). Prehnite has distinctive, sharp OH features, in particular at 1.48 μm and from 2.2 to 2.4 μm. The amphiboles indicative of higher degrees of metamorphism have similar spectra to one another but can be differentiated from minerals diagnostic of lower metamorphic grades. These spectral characteristics can be used to identify metamorphic grades from orbital data and, similarly, to identify minerals that provide evidence for hydrothermal alteration and diagenesis.

Identifying and mapping minerals on Mars

CRISM is a hyperspectral imaging spectrometer on the Mars Reconnaissance Orbiter (MRO) with 544 channels that sample the VNIR spectral region from 0.4 to 4.0 μm (Murchie *et al.*, 2007). CRISM operates in either a 72-channel mapping mode that will provide global coverage at 200 m/pixel or a full 544-channel targeted mode that provides 10 km × 10–20 km images at a resolution of 18–40 m/pixel. Spectral data from 1.0 to 2.6 μm in the latter, high-resolution mode are the focus of this paper and allow identification and mapping of mafic minerals and alteration minerals of most interest. (Note: CRISM images may be previewed and downloaded via a map search tool at http://crism.jhuapl.edu. The image IDs of all spectra shown are provided in short form in the figures with the leading four zeros omitted, *e.g.* image 454E is 0000454E.)

Prior to spectral analysis, atmospheric and photometric corrections were applied to CRISM data cubes to correct for viewing geometry and to separate out the contribution of reflected light from the surface from the effects of atmospheric transmission (Ehlmann *et al.*, 2009; Murchie *et al.*, 2009b). Following atmospheric correction, a noise-removal algorithm that removes data spikes in both the spectral and spatial domains but does not affect broader absorptions of mineralogic interest was implemented (Parente, 2008). In addition, to highlight spectral differences between areas and reduce residual atmospheric and instrumental artifacts in spectra, average spectra from regions of interest were divided by spectra from a dust-covered or otherwise spectrally unremarkable region in the same scene.

Once a particular mineral or group of minerals was identified, the spectral properties were parameterized and mapped spatially, *e.g.* by calculating absorption band depth for each pixel in an image (Pelkey *et al.*, 2007) or by more complex feature-fitting algorithms (Clark *et al.*, 2003). These mineral mapping techniques have been employed with success in terrestrial remote sensing, including in hydrothermal and metamorphic terrains (*e.g.* Kozak *et al.*, 2004; Brown *et al.*, 2005; Swayze *et al.*, 2009). The CRISM parameter maps were coregistered and combined with a variety of imaging datasets to obtain information about the geomorphology and geologic context of mineral detections. These include coordinated observations acquired by the two high-resolution MRO cameras, the Context Imager (CTX) and the High Resolution Imaging Science Experiment (HiRISE), which acquire images at 5 m/pixel and 0.25 m/pixel, respectively (Malin *et al.*, 2007; McEwen *et al.*, 2007). Collectively, information on diagnostic minerals and orbital data from Mars were used to identify numerous areas where evidence of likely low-grade metamorphic, hydro-thermal, or diagenetic activity is preserved.

https://doi.org/10.1346/CCMN.2011.0590402 Published online by Cambridge University Press

Table 2. Hydrated silicate minerals discovered on Mars through January, 2010. All mineral phases were observed from orbit using VNIR spectroscopy. Those which may serve as diagnostic indicator minerals for elevated temperatures and diagenesis, hydrothermal alteration, or low-grade metamorphism are indicated in the left-most column.

Indicator, elevated *T*	Hydrated silicate group/mineral	Formula	References
	Fe,Mg-smectites (*e.g.* nontronite, saponite)	$(Ca, Na)_{0.3\text{-}0.5}(Fe,Mg, Al)_{2-3}(Si, Al)_4O_{10}(OH)_2{\cdot}nH_2O$	Poulet *et al.* (2005); Mustard *et al.* (2008)
	Montmorillonite	$(Na,Ca)_{0.33}(Al,Mg)_2(Si_4O_{10})(OH)_2$	Poulet *et al.* (2005); Mustard *et al.* (2008)
	Kaolin-group minerals (*e.g.* kaolinite, halloysite)	$Al_2Si_2O_5(OH)_4$	Bishop *et al.* (2008); Ehlmann *et al.* (2009)
	Chlorite	$(Mg,Fe^{2+})_5Al(Si_3Al)O_{10}(OH)_8$	Mustard *et al.* (2008); Ehlmann *et al.* (2009)
√	Serpentine	$(Mg,Fe)_3Si_2O_5(OH)_4$	Ehlmann *et al.* (2009)
√	High-charge Al,K-phyllosilicate (*e.g.* illite or muscovite)	$(K,H_3O)(Al,Mg,Fe)_2(Al,Si)_4O_{10}(OH)_2$ [muscovite: $KAl_2AlSi_3O_{10}(OH)_2$]	Mustard *et al.* (2008); Ehlmann *et al.* (2009)
√	Prehnite	$Ca_2Al(AlSi_3O_{10})(OH)_2$	Clark *et al.* (2008); Ehlmann *et al.* (2009)
√	Analcime	$NaAlSi_2O_6{\cdot}H_2O$	Ehlmann *et al.* (2009)
	Opaline silica	$SiO_2{\cdot}H_2O$	Milliken *et al.* (2008); Ehlmann *et al.* (2009)

OBSERVATIONS

Mineralogy of the Martian surface

Hydrated silicate phases found on Mars to date (Table 2) are restricted to the southern highlands and Noachian terrains. Most are exposed by cratering, associated with thousands of craters across the southern highlands, although a few eroded escarpments (Nili Fossae, Mawrth Vallis, Valles Marineris, and Uzboi Vallis) provide excellent exposures of intact stratigraphic cross-sections. Regional surveys of cratered terrains in Terra Tyrrhena, Noachis Terra (Fraeman *et al.*, 2009), and west of the Isidis basin in northern Syrtis Major and near the Nili Fossae (Ehlmann *et al.*, 2009) were conducted to examine the prevalence and distribution of alteration mineral phases. These studies have shown that the most common alteration minerals are Fe,Mg-smectites (Figure 3; Mustard *et al.*, 2008). In a few instances, these smectites are accompanied by additional alteration phases. Chlorite-bearing or chlorite- and prehnite-bearing materials are the most common of these. Rarer are zeolites, hydrated silica, and illite (or muscovite). Serpentine has also been found and mapped on Mars, although it is uncommon (Ehlmann *et al.*, 2010b).

Fe,Mg-smectites can form in a wide range of terrestrial environments from pedogenic (*e.g.* weathering of basalt), to hydrothermal, to lacustrine precipitation, to direct precipitation from residual magmatic fluids (*e.g.* Meunier, 2005). Their detection on Mars indicates past aqueous processes occurring at neutral to alkaline pH but does not permit elucidation of the details of the conditions under which alteration took place (*e.g.* specific temperatures, pressures, or detailed fluid composition). As discussed above, other minerals can be more diagnostic of the pressure, temperature, and geochemical conditions at the time of formation. The locally diverse alteration minerals probably indicate locally distinctive aqueous processes. In particular, observations of four diagnostic minerals (or mineral assemblages) provide diagnostic evidence for alteration at elevated temperatures (Table 2).

Prehnite-bearing rocks

Prehnite occurs in multiple locations in ancient Martian cratered terrains (Clark *et al.*, 2008), including the greater Argyre basin region (Buczkowski *et al.*, 2010), the craters at the northern margin of Syrtis Major (Ehlmann *et al.*, 2009), and in Noachis Terra and Terra Tyrhenna (Fraeman *et al.*, 2009). Prehnite forms in hydrothermal or metamorphic conditions (*e.g.* Frey and Robinson, 1999) and has distinctive OH-related absorptions centered at 2.35 to 2.36 μm with additional weaker bands at 2.24 and 2.28 μm (Figure 2, 4). The principal VNIR absorption for prehnite coincides with the location of a 2.33 to 2.35 μm absorption found in chlorite, which

https://doi.org/10.1346/CCMN.2011.0590402 Published online by Cambridge University Press

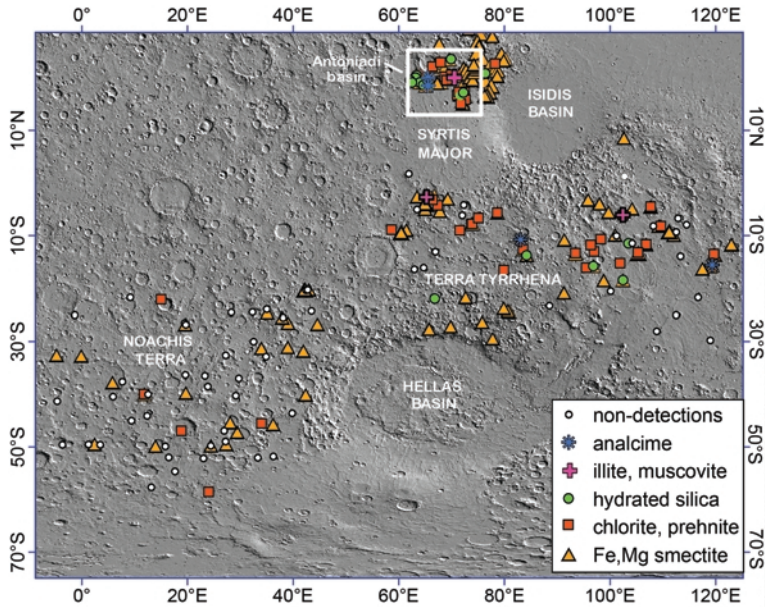

Figure 3. A Mars Orbiting Laser Altimeter (MOLA) hillshade map of the topography of Mars with mineral detections from a survey of CRISM targeted images overlain. Symbols represent minerals found within a CRISM image or group of images at a particular location (this spatial scale is too large to display the images). Fraeman *et al.* (2009) surveyed Noachis Terra and Terra Tyrrhena. Ehlmann *et al.* (2009) surveyed the area west of the Isidis basin. Fe,Mg-smectites are the most commonly detected alteration minerals, though localized instances of greater mineralogic diversity are observed. Examples for this review are taken from the area outlined by the white box.

makes it challenging to discriminate them remotely. However, prehnite has an OH overtone located at 1.48 μm, apparently unique among all other minerals (Clark *et al.*, 2007). Chlorite has a different, distinctive overall spectral shape and an OH overtone at 1.39 μm. The presence of the 1.48 μm absorption permits the unique determination of prehnite's presence. Interestingly, where found on Mars to date, prehnite is always in a mixture with chlorite.

Prehnite-bearing rocks are typically found associated with craters. For example, within a relatively fresh 40 km crater (near 16ºN, 72ºE), prehnite and chlorite are found along with silica and Fe,Mg-smectites (Figure 4; Ehlmann *et al.*, 2009). Nearly all of the rocks in and around the central peak of the crater are altered and numerous mixed pixels show attributes of multiple alteration minerals, *i.e.* mixtures of phases. Materials in the central peak are heavily brecciated and are excavated from depth (<4 km for a crater of this size, based on models by Melosh, 1989) by the impact process. Prehnite and chlorite are the areally most widespread phases based on analysis of CRISM targeted data for this crater. Silica (discussed further in the next section) is found in a few smaller areas in rocky knobs. All alteration minerals are found both in the crater central peak as well as in the wall rock and crater ejecta (Figure 4).

Analcime-silica-Fe,Mg-smectite-chlorite assemblages

Analcime forms in highly alkaline environments, either in saline-alkaline lakes or in low water:rock ratio hydrothermal alteration and metamorphism (*e.g.* Hay, 1986). Analcime is rarely found on Mars but a few craters north of the Hellas basin and in northern Syrtis Major near the Antoniadi Basin have collections of diverse alteration minerals which include analcime. Phases also commonly found near analcime-bearing materials include hydrated silica and Fe,Mg-smectite (Ehlmann *et al.*, 2009). Hydrated silica has been found in diverse geologic settings on Mars, including extensive layered deposits in and around Valles Marineris (Milliken *et al.*, 2008), small volcanic cone deposits (Skok *et al.*, 2010), and southern highlands craters (Ehlmann *et al.*, 2009). Silica forms at a variety of pHs and temperatures, and the presence of a silica phase is not, by itself, diagnostic of a formation environment (McLennan, 2003). Remote orbital VNIR spectroscopy can identify hydroxylated silica (the presence of Si-OH) and determine that a silica phase is hydrated (has structural H_2O) but not distinguish specific phases, *e.g.* opal *vs.* cherts *vs.* cristobalite. Hydrated silica has been found alone on Mars and in association with diverse phyllosilicates and sulfates. Where analcime has been found on Mars, silica has always been found in association.

A 25 km impact crater (20ºN, 66ºE) near the Antoniadi basin hosts diverse mineral deposits in and around the central peak (Figure 5; Ehlmann *et al.*, 2009). Fe,Mg-smectite and chlorite are detected using VNIR spectral data. Spectra of zeolite minerals are dominated by water-related absorptions, and analcime is identified

https://doi.org/10.1346/CCMN.2011.0590402 Published online by Cambridge University Press

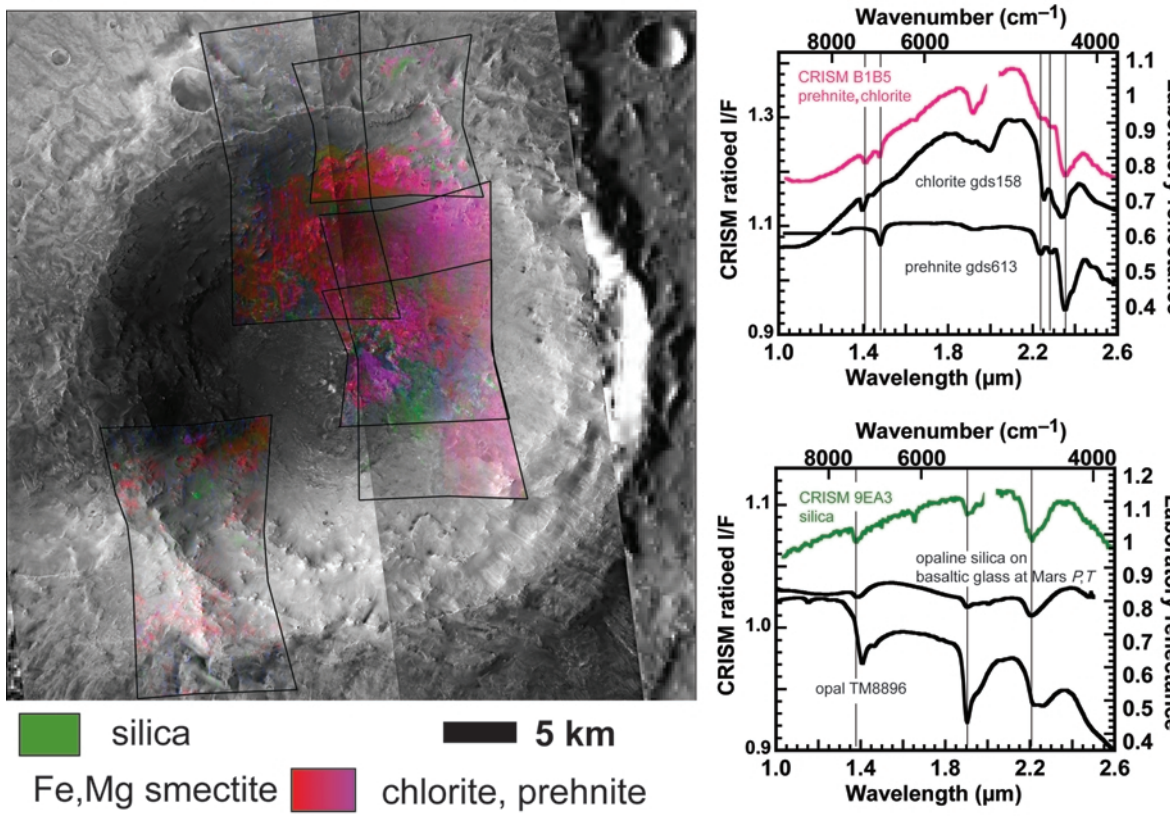

Figure 4. A 40 km crater in northern Syrtis major (16ºN, 72ºE) with prehnite-, chlorite-, and silica-bearing rocks. These minerals, together with Fe,Mg-smectite can be mapped in the crater walls, central peak, and ejecta. CRISM mineral maps were constructed by mapping absorption band depths at 2.3 μm (red), 2.2 μm (green), and 2.35 μm (blue) within targeted images (black outlines). Spectra characteristic of chlorite- and/or prehnite-bearing materials appear magenta, Fe,Mg-smectite red, and silica green in this color combination and display stretch. The color maps were overlain on a mosaic of CTX high-resolution images. CRISM spectral data from the color units were compared to data from laboratory samples (Clark *et al.*, 2007; Swayze *et al.*, 2007) and used to verify the mineral maps. Some pixels are composed of prehnite mixed with chlorite. Others have the distinctive signature of a hydrated silica phase. Laboratory spectra have been offset for clarity.

by strong, diagnostic absorptions at 1.42, 1.91, and 2.52 μm and a weaker absorption at 1.79 μm. Hydrated silica and hydrated basaltic glass share similar H_2O and Si-OH absorptions near 1.4, 1.9, and 2.2 μm. In hydrated silica (*e.g.* opaline phases, cherts, *etc.*), phases with more hydrogen-bonded H_2O have broader bands at these positions as is the case for silica-bearing materials in Figure 5 (also Figure 4; see Swayze *et al.*, 2007, Milliken *et al.*, 2008, for further discussion).

HiRISE data show that the central peak is highly brecciated with the largest blocks ~200 meters in diameter. Examination of spectral properties of CRISM pixels over large blocks *vs*. matrix materials did not reveal systematic spectral differences. The spectrally dominant alteration mineral in different areas of the central peak varies between analcime, Fe,Mg-smectite, and chlorite. Large-scale rippled sands of debris reworked by aeolian processes ring the central peak. These deposits host most of the hydrated silica. Additional spectral signatures of silica (and chlorite and smectite) are found in a few isolated knobs of rock on the crater wall. This is one of two craters in this region of Mars that possess the same mineral assemblage.

Chlorite- and illite- (or muscovite-) bearing materials

Chlorite is the second-most common class of phyllosilicate on Mars after Fe,Mg-smectite, and is often found mixed at a sub-pixel scale (<18 m/pixel) with prehnite-bearing materials (*e.g.* Figure 4) or in terrains associated with Fe,Mg-smectites. As discussed above, the spectral signature of chlorite is distinguished by its unique overall shape as well as absorptions at 1.39 μm and 2.33 to 2.35 μm and a shoulder at 2.26 μm (King and Clark, 1989). In pure specimens of chlorite, the 1.9 μm H_2O-related absorption is absent. On Earth, chlorite can be a primary mineral in felsic rocks and also forms *via* hydrothermal, metamorphic, and diagenetic reactions (*e.g.* Deer *et al.*, 2009).

The spectral signatures of the high interlayer-charge K,Al-phyllosilicates illite and muscovite have very

https://doi.org/10.1346/CCMN.2011.0590402 Published online by Cambridge University Press

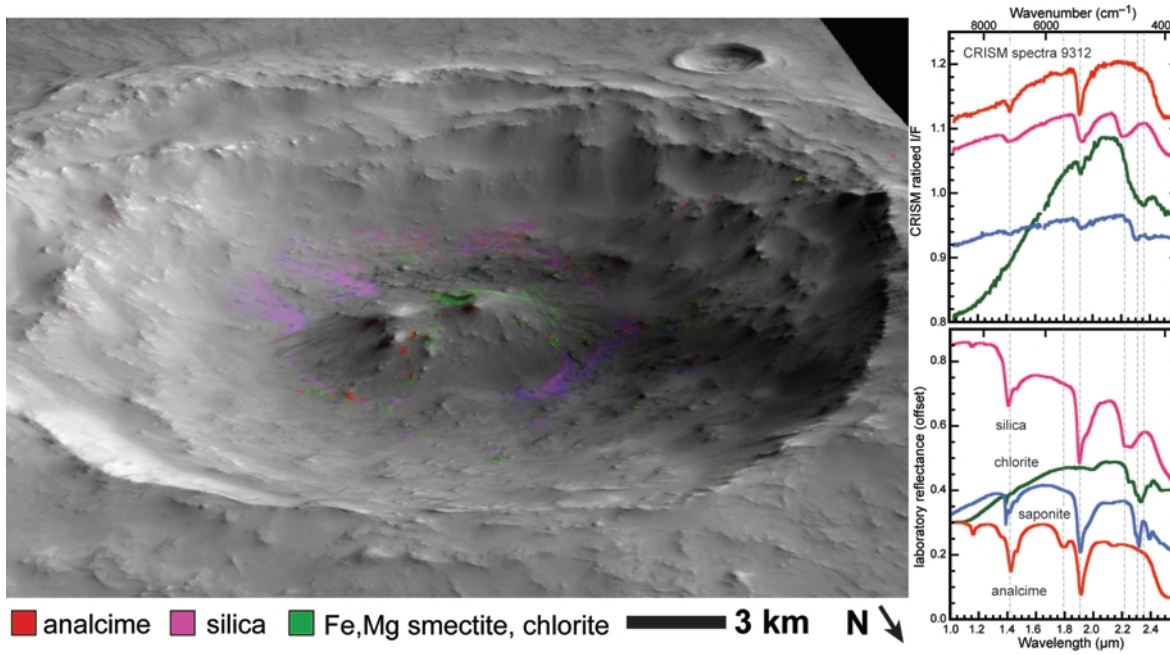

Figure 5. Analcime, silica, Fe,Mg-smectite, and chlorite have been identified in a 25 km impact crater in northern Syrtis Major (20ºN, 66ºE). CRISM mineral maps were constructed from the band depth at 2.5 μm (red), 2.3 μm (green), and 2.2 μm (blue) and the color mapping of minerals verified by comparing CRISM spectra to data from spectral libraries (Clark *et al.*, 2007). The maps were then overlain on a CTX image mosaic and draped over a MOLA-derived digital elevation model. In this color combination and display stretch, Fe,Mg-smectites and chlorite are both mapped in green, analcime is red, and silica is blue to magenta.

similar features at 1.40, 2.20, 2.35, and 2.44 μm (Kruse and Hauff, 1991) that cannot be distinguished at CRISM spectral resolution (Ehlmann *et al.*, 2009). Illite (or muscovite) is not commonly observed on Mars and is found in only a few impact craters (Fraeman *et al.*, 2009). Muscovite can form magmatically in felsic rocks or be formed as a product of hydrothermal alteration or metamorphism (Rosenberg, 2002). Illite can be formed by hydrothermal or diagenetic reactions, precipitation from highly alkaline-saline fluids, or by weathering of muscovite (Eberl *et al.*, 1993).

Chlorite- and illite (muscovite)-bearing materials are usually found together on Mars (Ehlmann *et al.*, 2009, 2010b). For example, the crater walls and ejecta of a 50 km crater (near 20ºN, 69ºE) exhibit the distinctive spectral signatures of these two minerals (Figures 6, 7). Alteration minerals are especially spatially widespread on the eroded eastern side of the crater, adjacent to the crater where ejecta would be deposited. The chlorite-bearing materials mapped here have some additional contribution from prehnite-bearing materials, as shown by the presence of the 1.48 μm absorption (Figure 6). The areally dominant materials in this crater's ejecta are chlorite- and prehnite-bearing. Illite (muscovite) occurs in small knobs comprising only a few CRISM pixels (Figure 7), yet its spectral signature can be isolated with careful analysis (Figure 6). Many pixels exist, the spectra of which show evidence of chlorite and illite (muscovite) mixed in variable proportions (Figure 6, middle spectrum of upper plot). The 2.35 μm absorption increases in strength as the chlorite component increases. No pixels are found with just a 2.2 μm absorption, as might be the case if the mineral responsible were another Al-phyllosilicate such as montomorillonite or kaolinite. As the 2.2 μm band increases in strength, the 2.35 μm band shows a correlated increase, also indicating that the single illite (muscovite) phase is the most probable explanation for the spectral data. The strongest absorptions are coincident with raised knobs and ridges (arrows in Figure 7). These spectral signatures become diffuse away from the knobs as mass wasting and eolian erosion transport and comminute the hydrated mineral-bearing materials and mix them with local dusts and soils.

Serpentine-bearing rocks

Serpentine has been identified on the surface of Mars in the ejecta and central peaks of craters, in association with other alteration minerals but with no obvious stratigraphy, and in an olivine-rich stratigraphic unit south of the Nili Fossae (Ehlmann *et al.*, 2010b). A distinctive spectral shape and four distinctive absorptions at 1.38, 2.11, 2.325, and 2.52 μm discriminate serpentine spectrally from other Martian alteration minerals (Figure 8e; Ehlmann *et al.*, 2010b). Serpentine results from the hydrothermal alteration of ultramafic rocks at temperatures ranging from just above ambient (Barnes and O'Neil, 1969) to ~400ºC (Evans, 2004). Fluids circulating

https://doi.org/10.1346/CCMN.2011.0590402 Published online by Cambridge University Press

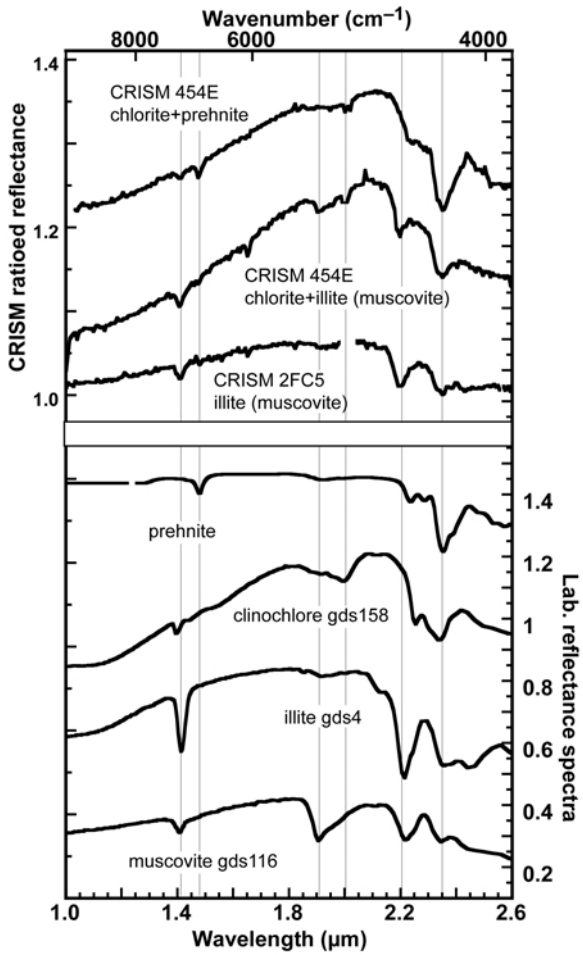

Figure 6. Spectral signatures of CRISM chlorite and prehnite and illite or muscovite and their mixtures compared to laboratory data from Clark *et al.* (2007). All spectra were taken from the images mapped in Figure 7.

in the rocks are of high pH, low $a_{SiO2,}$ and are typically highly reducing (Frost and Beard, 2007).

Serpentine, where it is found in stratigraphic sections, is associated with an olivine-rich unit (Figure 8; 17ºN, 77ºE), which has been mapped west and south of the 1900 km Isidis Basin, has a banded, fractured appearance, drapes underlying Fe,Mg-smectite clay rocks, and is estimated to have >~30 wt.% olivine (Hoefen *et al.*, 2003; Hamilton and Christensen, 2005; Mustard *et al.*, 2007, 2009). Here the olivine-rich unit is exposed beneath younger Hesperian lavas of the Syrtis Major formation. The olivine-rich unit is partially altered, in some locations exhibiting spectral signatures indicative of the presence of serpentine and in others exhibiting the spectral signature of magnesium carbonate, which is probably a weathering product from either the olivine or the serpentine (Figure 8; Ehlmann *et al.*, 2009, 2010b). To date, no other sites on Mars have been found where serpentine is part of a coherent statigraphy (further details are provided in Ehlmann *et al.*, 2010b).

DISCUSSION

Hydrothermal alteration/low-grade metamorphism of mafic and ultramafic rocks

Among the diverse alteration minerals mapped on Mars, prehnite provides the clearest evidence for aqueous alteration at elevated temperatures. Prehnite formation is restricted to a relatively narrow range of conditions (Figure 9). Thermodynamic and experimental data show it is a stable to metastable product at 200−400ºC and at <3kbar (a slightly greater range than shown on Figure 9a; Deer *et al.*, 1997; Robinson and Bevins, 1999; Schiffman and Day, 1999). In addition to temperature and pressure constraints, during prehnite formation, the mole fraction of CO_2 in the circulating fluids must be small, otherwise the Ca would be incorporated into calcite and prehnite would not form (Figure 9b; Robinson and Bevins, 1999). Calcite has thus far not been identified definitively in the southern highlands of Mars.

That no 'pure' prehnite VNIR spectral signatures appear at 18 m/pixel scale in the areas studied, and that it is always identified with chlorite, is also explained by examination of predicted metamorphic assemblages. At relatively low pressures and temperatures, <~400ºC, prehnite is expected to co-occur with chlorite (Figure 9a; Deer *et al.*, 1997; Schiffman and Day, 1999). Indeed, the prehnite, chlorite, and silica assemblage observed in the crater in Nili Fossae is an expected low-grade, low pCO_2 metamorphic assemblage, although whether the phases found are in thermodynamic equilibrium cannot be determined from orbit (Figure 9b).

At lower grades but with similar protoliths, analcime occurs as one of the minerals in zeolite-facies metamorphism (Figure 9a), and it is often accompanied by silica. Unlike prehnite, no lower temperature boundary exists for analcime formation, so its detection is not, by itself, sufficient as an indication that aqueous alteration must have occurred at elevated temperatures. Analcime precipitates from ~250ºC down to ambient temperatures in alkaline lake sediments where water interacts with detrital clay and volcanic glass (*e.g.* Hay, 1986). In lacustrine environments, the common mineral assemblage is clinoptilolite, erionite, analcime, and Na- and borosilicates (*e.g.* Eugster, 1980). In the analcime-bearing craters observed on Mars (*e.g.* Figure 5), however, the other hydrated silicates have not been found, and no evidence for lacustrine sedimentary units disrupted by cratering has been found. Rather, silica and Fe,Mg-smectites are the more common accompanying alteration minerals. Collectively, the morphologic and mineralogic evidence acquired to date is more indicative of diagenetic and hydrothermal settings for the formation of analcime on Mars. In Icelandic hydrothermal systems, for example, analcime is one of a suite of zeolites that serve as a 'geothermometer,' indicating temperatures of hydrothermal alteration between 75 and

https://doi.org/10.1346/CCMN.2011.0590402 Published online by Cambridge University Press

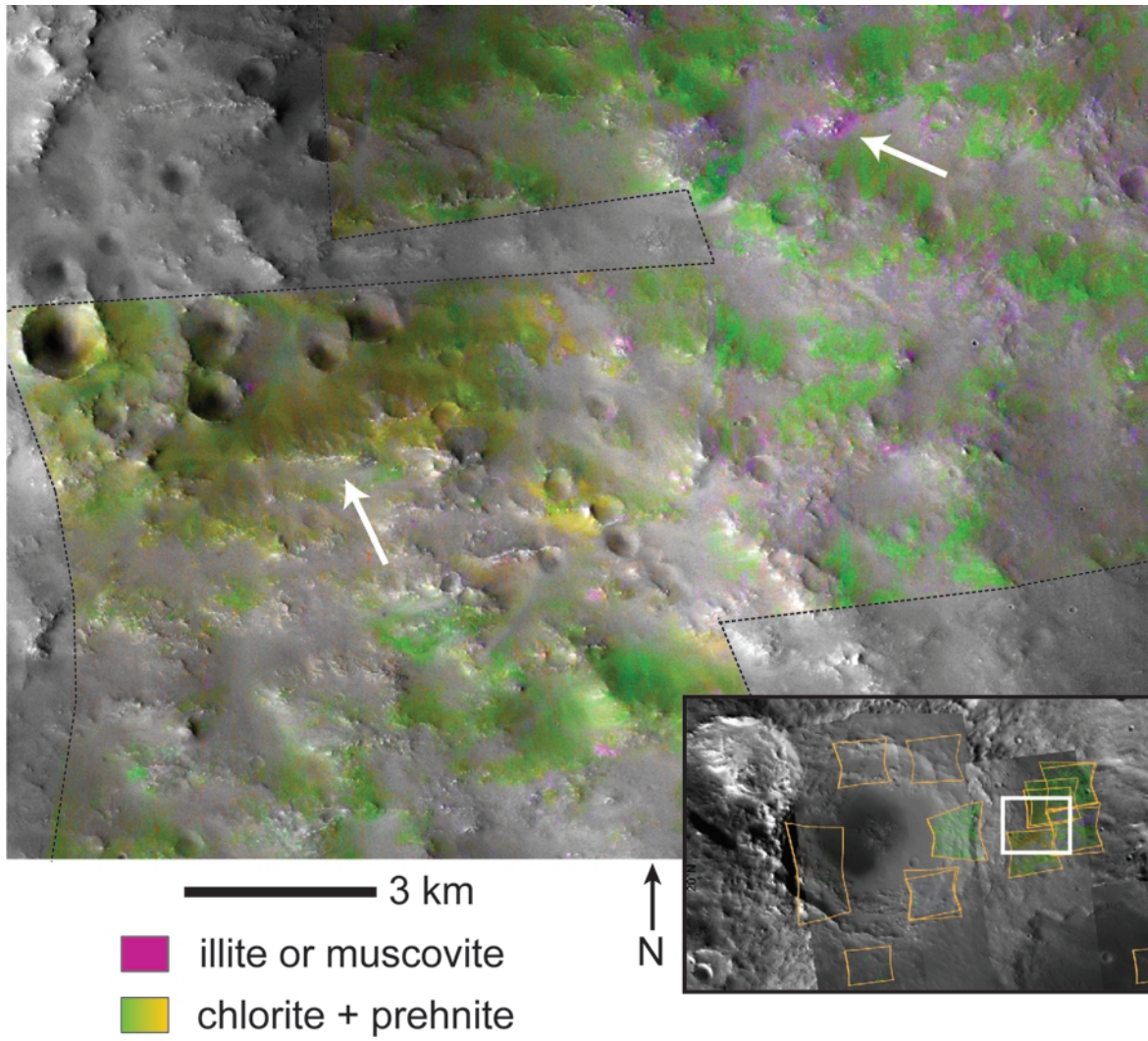

Figure 7. Chlorite, prehnite, and illite (or muscovite; see text) are found within and around a 50 km impact crater in northern Syrtis Major (20ºN, 69ºE). The inset shows the context of the larger image which was made from a composite of CRISM images acquired on the eastern side of the crater within the zone of impact ejecta deposition. CRISM mineral maps were constructed by mapping absorption band depths at 2.35 μm (red), 2.3 μm (green), and 2.2 μm (blue), stretched so that pixels with spectra characteristic of illite or muscovite are magenta and chlorite or prehnite yellow to green (for yellow areas, the 2.35 μm absorption is sharper). These were overlain on a CTX image mosaic. The strongest mineral signatures coincide with rocky knobs and ridges (*e.g.* white arrows) and become weaker with distance from these knobs. Spectra from these CRISM images are shown in Figure 6 and were used to verify the color mapping of the mineralogy.

225ºC in altered basalts (Wiesenberger and Selbekk, 2008). In drill holes in volcaniclastic sediments, analcime crystallizes at 70–90ºC (Velde and Iijima, 1988). In both of these terrestrial settings, analcime is commonly accompanied by Fe,Mg-smectites, chlorites, silica, and other zeolites.

The VNIR spectral signatures and morphologic settings of the prehnite-chlorite-silica and analcime-silica-Fe,Mg-smectite-chlorite assemblages are best explained by alteration of basaltic rocks at elevated temperatures. The temperatures and pressures implied are at the boundary of what is variously termed low-grade metamorphism or hydrothermal alteration, depending on the fluid source and water:rock ratio. Regardless of the terminology used, the mineralogy implies alteration at elevated temperatures above 200ºC but probably below 400ºC. The pressures probably do not exceed 3 kbar (Figure 9). Where serpentine is found instead, the pressure and temperature conditions implied are the same, although the ultramafic, as opposed to mafic, precursor host rocks generate different fluid compositions and, consequently, precipitation of different alteration minerals (Ehlmann *et al.*, 2010b). During metamorphism, lower a_{SiO2} and a_{CaO} means serpentine

https://doi.org/10.1346/CCMN.2011.0590402 Published online by Cambridge University Press

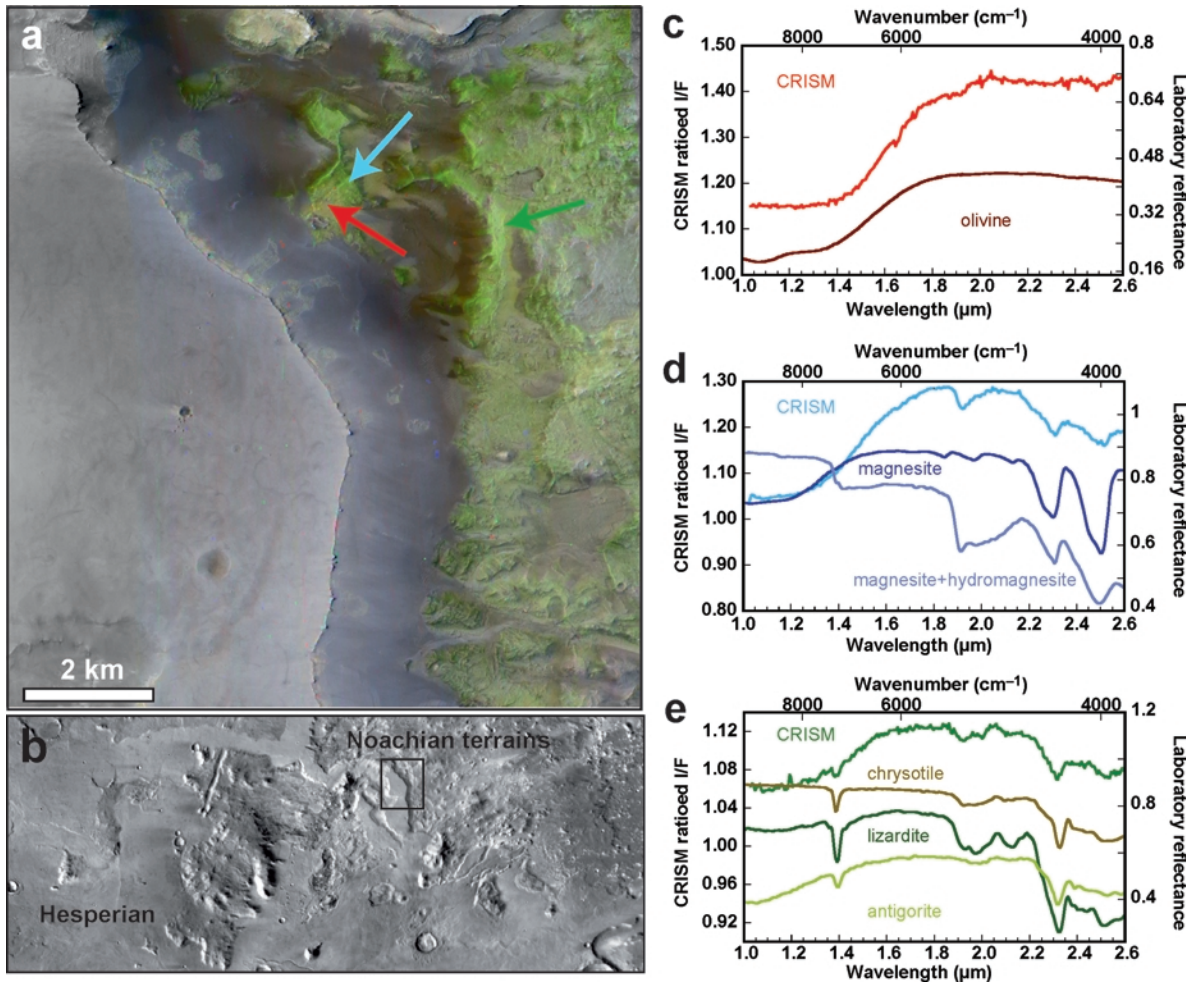

Figure 8. Serpentine in a stratigraphic section in northern Syrtis Major (17ºN, 77ºE). Serpentine is found associated with an olivine-rich unit that is variably altered to Mg carbonate and serpentine. (a) A subset of CRISM image B8C2 in false color (red: 2.38, green: 1.80, blue: 1.15 μm) shows the olivine-rich unit (yellow-green) beneath younger lavas (dark purple unit on the left side of image). (b) Context: this CRISM image covers part of the eastern boundary of the lava flows. (c–e) Ratioed CRISM spectra extracted from the locations indicated by the color-coded arrows in (a) compared to library data from the CRISM spectral library and Clark *et al.* (2007) allow discrimination of olivine, Mg-carbonate, and serpentine within the rock unit.

is favored over chlorite and prehnite (Frost and Beard, 2007). Magnesium-carbonate may form in the same hydrothermal system as serpentine when fluids are in communication with the CO_2-rich atmosphere or, alternatively, as a later weathering product (Barnes and O'Neil, 1969; Ehlmann *et al.*, 2008, 2010).

No amphiboles indicative of higher pressure (blueschist) or higher temperature (greenschist) metamorphic facies have been found, even though these phases are infrared active and would be detected by CRISM if present at sufficient abundance in the rock at an 18 m/pixel scale in the areas surveyed (Figure 2). The apparent absence of assemblages spectrally dominated by actinolite-epidote and hornblende suggests that higher-grade metamorphism has not been an important process in Mars history, a conclusion that makes sense given the absence of the typical tectonic settings (convergent plate margins) in which these minerals form on Earth. The transient high heats and pressures of impact may be insufficiently long-lived for these minerals to form (Schwenzer and Kring, 2009). An alternative is that, given Mars' lower gravity than Earth's, greater depths are required to reach the pressures for blueschist-facies amphibole formation (Figure 1), and materials at these depths are rarely excavated by cratering.

Rocks that have the spectral signatures observed in and around the southern highlands craters discussed here need not be composed primarily of alteration minerals and instead are probably similar to common hydrothermally altered basalts from Earth (Figure 10). In these basaltic rocks, fluid flow through vugs and fractures has

https://doi.org/10.1346/CCMN.2011.0590402 Published online by Cambridge University Press

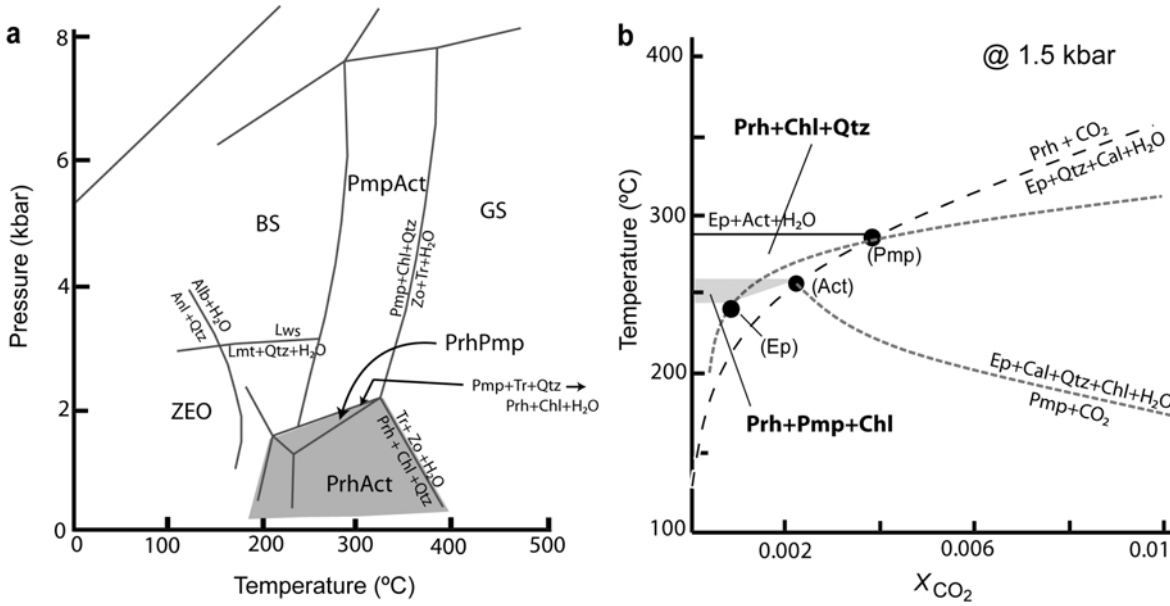

Figure 9. (a) Phase diagrams indicating prehnite stability as functions of temperature and pressure. Metamorphic facies (ZEO = zeolite, GS = greenschist, BS = blueschist) are indicated and selected reactions are shown (adapted from Schiffman and Day, 1999). (b) Temperature and mole fraction of CO_2 (adapted from Robinson and Bevins, 1999). Prh = prehnite, Pmp = pumpellyite, Chl = chlorite, Anl = analcime, Qtz = quartz, Alb = albite, Lws = lawsonite, Zo = zoisite, Tr = tremolite, Ep = epidote, Act = actinolite, Cal = calcite.

resulted in mineralization of zeolites and prehnite-pumpellyite while the bulk rock itself is only weakly altered (usually to Fe,Mg-smectite and mixed-layer chlorite/smectite). When VNIR spectral signatures of altered basalts are ratioed to unaltered basalts, the VNIR spectral signatures of the alteration minerals will be prominent, even though they may comprise only a small portion of the surface area. Differential weathering of the altered rock may serve to concentrate certain precipitated phases depending on their relative resistances to physical and chemical weathering. For example, when subjected to aeolian erosion and transport, precipitated silica nodules will be resistant to breakdown due to their hardness. Silica would tend to remain behind as a lag while clays and zeolites are broken down into finer-grained particles which can be removed by transport. As previously noted by Ehlmann *et al.* (2009), this may explain the occurrence of silica in aeolian deposits ringing the central peak of the 25 km crater in Figure 5 and may also explain the occurrence of

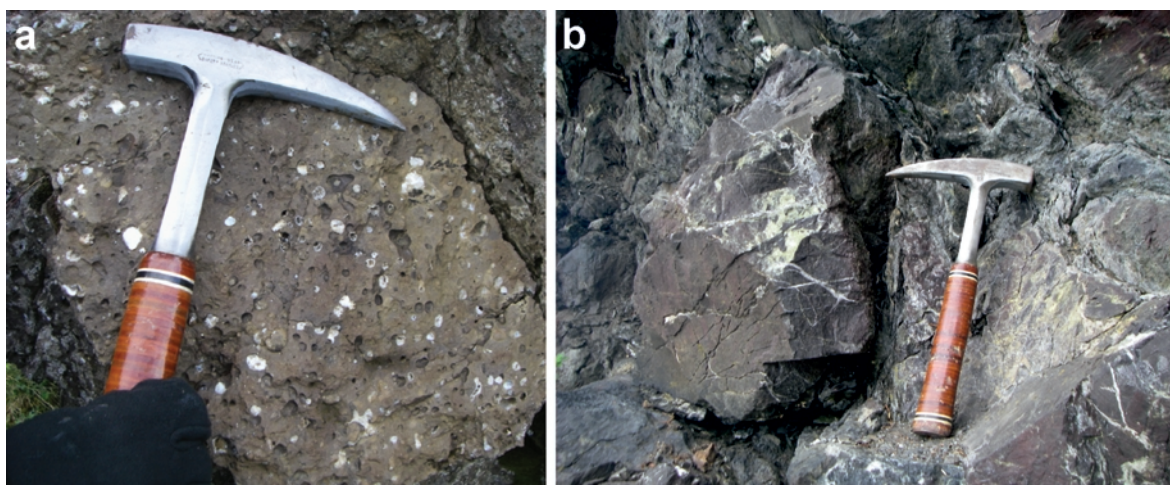

Figure 10. Basaltic rocks altered by hydrothermal activity/low-grade metamorphism. (a) Zeolitized rocks from western Iceland. (b) Prehnite/pumpellyite and silica precipitation in basalts from the Bay of Islands ophiolite in Newfoundland.

https://doi.org/10.1346/CCMN.2011.0590402 Published online by Cambridge University Press

zeolites in the dust of Mars (Ruff, 2004). Alternatively, the hydrated silica might be explained by the aqueous weathering of glassy impactites.

Diagenesis

On Earth, smectites rarely persist in the long-term rock record because diagenetic processes transform these clays, at least partially, to illite or chlorite (*e.g.* Hower *et al.*, 1976; Ahn and Peacor, 1985; Środoń, 1999; Meunier, 2005). That smectite clays and not illite are the predominant clays on Mars, persisting to the present in spite of burial, has been used to argue that the integrated contact time of these rocks and sediments with fluids must be short (Tosca and Knoll, 2009). However, sufficient K^+ activities are also required for the smectite-to-illite transformations to occur and, as discussed below, evidence of chlorite, a possible, and perhaps more probable, product of the diagenetic maturation of Fe,Mg-smectite, is widespread.

So far, the detection of illite (muscovite) has been rare on Mars and restricted to disrupted strata. In the case of the 50 km crater in Figure 7, the detections of alteration minerals are closely associated with knobby topographic highs. The complex geologic setting makes the origin of the rocks bearing the illite (muscovite) signature difficult to ascertain. The knobs may result from fluid flow in conduits which became mineralized and more resistant to the subsequent erosion that has stripped away surrounding and overlying materials. Alternatively, the knobs may be part of the materials in the crater's ejecta, *i.e.* rocks that have been excavated from depths of <5 km by this impact and then eroded differentially. In either case, rocks from depth have been exposed.

On Earth, muscovite can be primary in granitic terrains and then weather to illite. However, on Mars, where basalt is dominant, illite (muscovite) probably results from hydrothermal activity or diagenesis. For dioctahedral smectites, the most common way of forming illites is by diagenesis, which begins upon burial, usually as temperatures reach 50–80ºC. For aluminous clays, when K is sufficiently available in the environment, illite phases become more ordered with temperature and time with smectites converting to mixed-layer illite-smectite clays and then illites (Hower *et al.*, 1976). For trioctahedral smectites, the reaction proceeds instead through chlorite-smectite mixed layers to chlorite (Merriman and Peacor, 1999). In contrast to the rarity of illite (muscovite), chlorite is a common phyllosilicate on Mars (Figure 3).

In the broader region extending far from this 50 km crater, Fe,Mg-smectites are the dominant alteration minerals, found in breccias and in sedimentary deposits (Ehlmann *et al.*, 2009; Figure 3). Kaolin-group minerals occupy a thin unit capping the Fe,Mg-smectites (see Ehlmann *et al.*, 2009 for further discussion). The chlorite- and illite (muscovite)-bearing materials found east of this 50 km crater (Figure 7) and at other craters may have formed by the diagenesis of these Fe-, Mg-, and Al-clay-bearing units at depth with the relative proportions determined by the relative proportions of precursor clay minerals. That is, the kaolin-family mineral may have transformed to illite and the Fe,Mg-smectite to chlorite. Given the predominance of Fe,Mg-smectites on Mars, chlorite would be expected to dominate a diagenetic assemblage because of the Fe,Mg-rich precursor mineral and the paucity of K^+ needed to form illite. Chlorite and illite (muscovite) may thus be indicators of diagenetic activity on Mars, although a hydrothermal origin or lower-temperature formation from highly alkaline-saline fluids cannot be excluded.

Timing of mineral formation relative to cratering

Most of the exposures of diagnostic minerals and mineral assemblages are in craters rather than exposed in intact stratigraphic sections, complicating interpretation of the geologic setting of alteration. In the cratering process, materials at depth are excavated ballistically and deposited around the crater (*e.g.* Barnhart and Nimmo, 2011) as well as brought up from depths of ~$1/10^{th}$ (fraction) of the crater diameter during central peak formation (*e.g.* Melosh, 1989). When associated with craters, a key question is the timing of mineral formation. Did the low-grade metamorphic/hydrothermal processes pre-date or post-date formation of the impact craters? Modeling shows that post-impact hydrothermal activity is restricted to the subsurface beneath a crater, and only if a crater lake is sustained do waters reach the surface (Rathbun and Squyres, 2002; Abramov and Kring, 2004; Barnhart *et al.*, 2010). Hence, minerals in crater walls and ejecta presumably formed prior to the cratering event (Figure 11). If materials in the central peak differed from these, hydrothermal systems after impact may be implicated. In a post-impact hydrothermal-system scenario, the mineralogy of the crater's central region would differ from the rest of the materials because the minerals form in a different thermal and geochemical environment (Figure 11). However, in craters to date, differences in mineralogy interior and exterior to the crater have not been observed. Hence, alteration minerals discussed here probably formed prior to impact, and cratering serves only as a mechanism to create exposure.

Outstanding questions

As CRISM continues to map the surface of Mars, more exposures of diverse mineral assemblages may yet be found that provide further insights into the conditions of aqueous alteration. Certainly, heat and water were available on ancient Mars to generate the low-temperature and low-pressure hydrothermal, metamorphic, and possibly diagenetic conditions in many geographic areas, including those reviewed here. A key advance in

https://doi.org/10.1346/CCMN.2011.0590402 Published online by Cambridge University Press

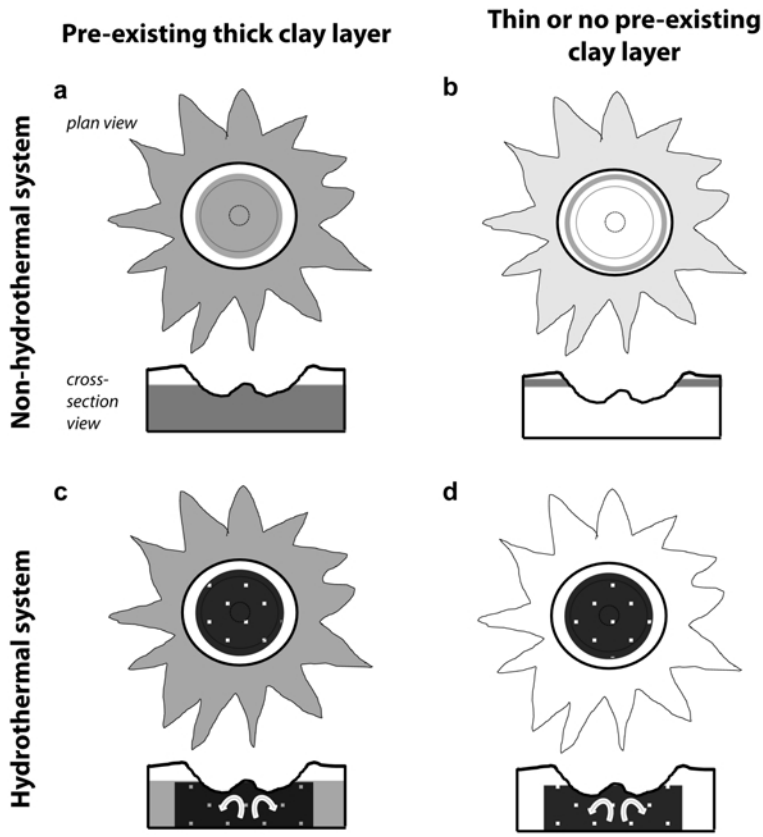

Figure 11. Schematic illustration of the mineral distribution around a crater expected as a result of the existence of a buried clay mineral-bearing stratum, a post-impact hydrothermal system, or both. Panels show the expected distribution for cratering (a) disturbing a thick, pre-existing clay layer, (b) disturbing a thin, pre-existing clay layer, (c) disturbing a thick, pre-existing clay layer with later post-impact hydrothermal activity, and (d) with later post-impact hydrothermal activity only. Minerals formed in a hydrothermal system (dark with white circles) would differ from pre-existing clays (gray). To date, only instances of clays with distribution like that in (a) and (b) have been found on Mars.

interpretation of VNIR spectra would be the ability to discern remotely the presence of mixed-layer clays, such as illite-smectite and chlorite-smectite minerals which indicate diagenesis. Some progress is being made in this regard for remote detection (Milliken *et al.*, 2010), and instruments on landed missions could also allow more detailed mineralogic characterization.

Cooling of Mars' early crust (Parmentier and Zuber, 2007), heat from impacts (Newsom, 1980), or heat from volcanic flows, *e.g.* Syrtis Major, may have supplied the heat necessary for the observed low-grade metamorphism or hydrothermal alteration. If the alteration minerals formed during crustal cooling, minerals would have precipitated in a stratified way controlled by depth, *i.e.* with the stratification of phases governed by the geothermal gradient and pressure, *e.g.* zeolites shallow, prehnite deeper, and amphiboles deeper still. Interestingly, the diagnostic minerals mapped so far appear to show no characteristic stratification with depth or differences in materials excavated as a function of crater diameter (larger craters excavate materials originally deeper in the crust) (Fraeman *et al.*, 2009). This suggests either that crustal cooling was not the mechanism responsible or that repeated regolith churning by impacts into the crust has destroyed evidence for mineral stratification. The mineral assemblages found also do not appear to have any strong geographic regional dependencies (Figure 3). For example, the craters shown in Figures 4–6 are all within ~500 km of each other yet exhibit strikingly different mineral assemblages. Controls on the spatial distribution of alteration minerals are not well understood at this time.

While excavation of minerals from depth is the simplest explanation of the distribution of minerals around craters, the question of timing is not fully settled. The effects of shock from high heat and pressure during impact on transformation of clays are not understood, *i.e.* whether they survive; nor are the mineralogies that might result from alteration of hot ejecta. Resolving these questions definitely will require the merging of results from laboratory experimentation, high-resolution models of impact-cratering processes (*e.g.* Abramov and

https://doi.org/10.1346/CCMN.2011.0590402 Published online by Cambridge University Press

Kring, 2005), and geochemical models (thermodynamic and kinetic) for mineral formation (*e.g.* Schwenzer and Kring, 2009) and destruction. By coupling detailed knowledge of temperature and mass movement with understanding of mineral formation/destruction rates, the question of pre- or post-impact alteration can be assessed rigorously.

This question is important for understanding the timing and duration of aqueous activity on early Mars. Was hydrothermal activity restricted to the Noachian (>3.7 Gy) and the time of impact-basin formation and initial crustal cooling? In this instance, alteration minerals excavated by craters are exposed at later times, but hydrothermal systems were only active very early in the planet's history. The alternative is hydrothermal alteration, possibly related to small impacts or perhaps to emplacement of volcanic flows extending from the Noachian into the Hesperian period of Mars (>2.7 Gy). Such longevity would bode well for the sustenance of habitatable environments through time. Terrestrial hydrothermal systems host diverse microbial communities, including some of the most deeply rooted (ancient) organisms on the phylogenic tree. Intact, coherent stratigraphies of Martian hydrothermal alteration (*e.g.* Figure 8) represent prime targets for future landed missions searching for biosignatures or mineralized organic matter (*e.g.* Farmer, 1996).

SUMMARY AND IMPLICATIONS

Some of the hydrated silicate minerals detected on Mars by CRISM VNIR imaging spectroscopy indicate the temperature of aqueous alteration and suggest hydrothermal and/or low-grade metamorphic formation conditions. Prehnite provides definitive evidence for alteration at higher temperatures (200–400ºC) and typically co-occurs in association with chlorite and silica. Analcime commonly occurs in assemblages with silica and Fe,Mg-smectite. In these assemblages, analcime probably indicates hydrothermal alteration, although at somewhat lower temperatures (50–200ºC) than indicated by prehnite-bearing assemblages. Serpentine indicates similar temperature conditions of alteration (<400ºC) but of ultramafic rather than mafic precursor rock. Finally, the occurrence of illite (or muscovite) in association with chlorite-bearing materials may be the product of diagenesis (<100ºC) of smectite-bearing sediments. In all cases, the alteration conditions implicated are low-grade. High-temperature and pressure phases indicating higher grades of metamorphism have not been found on Mars. Key outstanding questions include the nature of the processes that generated the hydrothermal environment (*e.g.* source of heat) and their timing. Further studies of the nature, timing, and longevity of Martian hydrothermal systems will enable understanding of how the availability of liquid water and planetary habitability changed through time.

REFERENCES

Abramov, O. and Kring, D.A. (2005) Impact-induced hydrothermal activity on early Mars. *Journal of Geophysical Research*, **110**, E12S09, doi:10.1029/2005JE002453.

Ahn, J.H. and Peacor, D.R. (1985) Transmission electron microscopic study of diagenetic chlorite in Gulf Coast argillaceous sediments. *Clays and Clay Minerals*, **33**, 228–237.

Allen, C.C., Gooding, J.L., and Keil, K. (1982) Hydrothermally altered impact melt rock and breccia: Contributions to the soil of Mars. *Journal of Geophysical Research*, **87**(B12), 10,083–10,101, doi: 10.1029/JB087iB12p10083.

Andrews-Hanna, J.C., Phillips, R.J., and Zuber, M.T. (2007) Meridiani Planum and the global hydrology of Mars. *Nature*, **446**, 163–166.

Arkai, P., Sassi, F.P., and Desmons, J. (2003) A systematic nomenclature for metamorphic rocks. 5. Very low- to low-grade metamorphic rocks. *Recommendations by the IUGS Subcommission on the systematics of metamorphic rocks*. SCMR website (www.bgs.ac.uk/SCMR).

Barnes, I. and O'Neil, J.R. (1969) The relationship between fluids in some fresh alpine-type ultramafics and possible modern serpentinization, Western United States. *Geological Society of America Bulletin*, **80**, 1947–1960.

Barnhart, C.J. and Nimmo, F. (2011) Role of impact excavation in distributing clays over Noachian surfaces. *Journal of Geophysical Research*, **116**, E01009.

Barnhart, C.J., Nimmo, F., and Travis, B.J. (2010) Martian post-impact hydrothermal systems incorporating freezing. *Icarus*, **208**, 101–117.

Bibring, J.-P., Langevin, Y., Gendrin, A., Gondet, B., Poulet, F., Berthe, M., Soufflot, A., Arvidson, R., Mangold, N., Mustard, J., Drossart, P., and the OMEGA team (2005) Mars surface diversity as revealed by the OMEGA/Mars Express Observations. *Science*, **307**, 1576–1581.

Bibring, J.-P., Langevin, Y., Mustard, J., Poulet, F., Arvidson, R., Gendrin, A., Gondet, B., Mangold, N., Pinet, P., Forget, F., and the OMEGA team (2006) Global mineralogical and aqueous Mars history derived from OMEGA/Mars Express data. *Science*, **312**, 400–404.

Bishop, J., Pieters, C., and Edwards, J.O. (1994) Infrared spectroscopic analyses on the nature of water in montmorillonite. *Clays and Clay Minerals*, **42**, 702–716.

Bishop, J., Madejová, J., Komadel, P., and Froschl, H. (2002a) The influence of structural Fe, Al, and Mg on the infrared OH bands in spectra of dioctahedral smectites. *Clay Minerals*, **37**, 607–616.

Bishop, J.L., Murad, E., and Dyar, M.D. (2002b) The influence of octahedral and tetrahedral cation substitution on the structure of smectites and serpentines as observed through infrared spectroscopy. *Clay Minerals*, **37**, 617–628.

Bishop, J.L., Noe Dobrea, E.Z., McKeown, N.K., Parente, M., Ehlmann, B., Michalski, J., Milliken, R.E., Poulet, F., Swayze, G., Mustard, J., Murchie, S., and Bibring, J.-P. (2008) Phyllosilicate diversity and past aqueous activity revealed at Mawrth Vallis, Mars. *Science*, **321**, 830 – 833, doi:10.1126/science.1159699.

Brown, A., Walter, M.R., and Cudahy, T.J. (2005) Hyperspectral imaging spectroscopy of a Mars analogue environment at the North Pole Dome, Pilbara Craton, Western Australia, *Australian Journal of Earth Sciences*, **52**, 3353–3364.

Buczkowski, D.L., Murchie, S., Clark, R., Seelos, K., Seelos, F., Malaret, E., and Hash, C. (2010) Investigation of an Argyre basin ring structure using Mars Reconnaissance Orbiter/Compact Reconnaissance Imaging Spectrometer for Mars. *Journal of Geophysical Research*, **115**, E12011, doi:10.1029/2009JE003508.

Cann, J.R. (1979) Metamorphism in the ocean floor. Pp. 230–238 in: *Deep Sea Drilling Results in the Atlantic Ocean: Ocean Crust, 2nd Ewing Symposium* (C.G.A. Harrison and D.E. Hays, editors). American Geophysical Union, Washington, D.C.

Chen, C.H., Chu, H.T., Liou, J.G., and Ernst, W.G. (1983) Explanatory notes for the metamorphic facies map of Taiwan. *Special Publication of the Central Geological Survey*, **2**, 1–32.

Clark, R.N. (1999) Spectroscopy of Rocks and Minerals, and Principles of Spectroscopy. Pp. 3–58 in: *Manual of Remote Sensing*, Volume 3, *Remote Sensing for the Earth Sciences* (A.N. Rencz, editor). John Wiley and Sons, New York.

Clark, R.N., King, T.V.V., Klejwa, M., Swayze, G.A., and Vergo, N. (1990) High spectral resolution reflectance spectroscopy of minerals. *Journal of Geophysical Research*, **95**, 12,653–12,680, doi:10.1029/JB095iB08p12653.

Clark, R.N., Swayze, G.A., Livo, K.E., Kokaly, R.F., Sutley, S.J., Dalton, J.B., McDougal, R.R., and Gent, C.A. (2003) Imaging spectroscopy: Earth and planetary remote sensing with the USGS Tetracorder and expert systems. *Journal of Geophysical Research*, **108**(E12), 5131, doi: 10.1029/2002JE001847.

Clark, R.N., Swayze, G.A., Wise, R., Livo, K.E., Hoefen, T.M., Kokaly, R.F., and Sutley, S.J. (2007) USGS Digital Spectral Library splib06a. *U.S. Geological Survey Data*, 231.

Clark, R.N., Swayze, G., Murchie, S., Mustard, J., Milliken, R., Ehlmann, B., McKeown, N., Calvin, W., Wray, J., and Bishop, J. (2008) Diversity of mineralogy and occurrences of phyllosilicates on Mars. *Eos Transaction of the American Geophysical Union*, **89**(53), Fall Meeting Supplement, Abstract P43D-04.

Cloutis, E.A., Asher, P.M., and Mertzman, S.A. (2002) Spectral reflectance properties of zeolites and remote sensing implications. *Journal of Geophysical Research*, 107(E9), 5067, doi:10.1029/2000JE001467.

Coombs, D.S., Ellis, A.J., Fyfe, W.S., and Taylor, A.M. (1959) The zeolite facies, with comments on the interpretation of hydrothermal syntheses. *Geochimica et Cosmochimica Acta*, **17**, 53–107.

Deer, W.A., Howie, R.A., and Zussman, J. (1997) *Rock Forming Minerals, vol 2: Double Chain Silicates*. 2nd edition. The Geological Society, London, 764 pp.

Deer, W.A., Howie, R.A., and Zussman, J. (2009) *Rock Forming Minerals, vol 3B: Layered Silicates Excluding Micas and Clay Minerals*. 2nd edition. The Geological Society, London, 320 pp.

Eberl, D.D., Velde, B., and McCormick, T. (1993) Synthesis of illite-smectite from smectite at Earth surface temperatures and high pH. *Clay Minerals*, **28**, 49–60.

Ehlmann, B.L. *et al.* (2008) Orbital identification of carbonate-bearing rocks on Mars. *Science*, **322**, 1828–1832.

Ehlmann, B.L., Mustard, J., Swayze, G., Clark, R., Bishop, J., Poulet, F., Des Marias, D., Roach, L., Milliken, R., Wray, J., Barnouin-Jha, O., and Murchie, S. (2009) Identification of hydrated silicate minerals on Mars using MRO-CRISM: Geologic context near Nili Fossae and implications for aqueous alteration. *Journal of Geophysical Research*, **114**, E00D08, doi:10.1029/2009JE003339.

Ehlmann, B.L., Mustard, J.F., Bish, D.L., and Poulet, F. (2010a) How much clay is on Mars? Lessons from visible/near-infrared (VNIR) and XRD study of hydrated silicate mineral assemblages in altered basalts from Iceland. The First Moscow Solar System Symposium, conference abstract, Moscow, October 11–15, 2010.

Ehlmann, B.L., Mustard, J.F., and Murchie, S.L. (2010b) Geologic setting of serpentine-bearing rocks on Mars. *Geophysical Research Letters*, **37**, L06201, doi: 10.1029/2010GL042596.

Eugster, H.P. (1980) Geochemistry of evaporitic lacustrine deposits. *Annual Reviews of Earth and Planetary Science*, **8**, 35 – 63, doi: 10.1146/annurev.ea.08.050180.000343.

Evans, B.W. (2004) The serpentine multisystem revisited. Pp. 5–32 in: *Serpentine and Serpentinites* (W.G. Ernst, editor). Geological Society of America, Columbia, Maryland.

Farmer, J. (1996) Hydrothermal systems on Mars: An assessment of present evidence. Pp. 273–299 in: *Evolution of Hydrothermal Ecosystems on Earth (and Mars?).* John Wiley, New York.

Fassett, C.I. and Head, J.W. (2008) Valley network-fed, open-basin lakes on Mars: distribution and implications for Noachian surface and subsurface hydrology. *Icarus*, **198**, 37–56.

Fleet, M.E. and Howie, R.A (2006) *Rock Forming Minerals, vol. 3A: Micas*. Geological Society, London, 780 pp.

Fraeman, A.A., Mustard, J., Ehlmann, B., Roach, L., Milliken, R., and Murchie, S. (2009) Evaluating models of crustal cooling using CRISM observations of impact craters in Terra Tyrrhena and Noachis Terra. *Lunar and Planetary Science Conference*, **40**, abstract 2320.

Frey, M. and Robinson, D. (1999) *Low-Grade Metamorphism*. Blackwell Science, Oxford, UK, 313 pp.

Frost, B.R., and Beard, J.S. (2007) On silica activity and serpentinization. *Journal of Petrology.*, **48**, 1351–1368.

Gaffey, S.J. (1987) Spectral reflectance of carbonate minerals in the visible and near infrared (0.35–2.55 um): anhydrous carbonate minerals. *Journal of Geophysical Research*, **92**, 1429–1440.

Gendrin, A., Mangold, N., Bibring, J.-P., Langevin, Y., Gondet, B., Poulet, F., Bonello, G., Quantin, C., Mustard, J., Arvidson, R., and LeMouelic, S. (2005) Sulfates in Martian layered terrains: the OMEGA/Mars Express View. *Science*, **307**, 1587–1591.

Gooding, J.L. (1992) Soil mineralogy and chemistry on Mars: possible clues from salts and clays in SNC meteorites. *Icarus*, **99**(1), 28–41.

Griffith, L.L. and Shock, E.L. (1997) Hydrothermal hydration of Martian crust: Illustration via geochemical model calculations. *Journal of Geophysical Research*, **102**(E4), 9135–9143.

Gulick, V.C. and Baker, V.R. (1990) Origins and evolution of valleys on Martian volcanoes. *Journal of Geophysical Research*, **95**, 14325–14344.

Hamilton, V.E. and Christensen, P.R. (2005) Evidence for extensive, olivine-rich bedrock on Mars. *Geology*, **33**(6), 433–436.

Harvey R.P. and McSween Jr., H.Y. (1996) A possible high-temperature origin for the carbonates in the Martian meteorite ALH84001. *Nature*, **382**, 49–51

Hay, R.L. (1986) Geologic occurrence of zeolites and some associated minerals. *Pure and Applied Chemistry*, **58**, 1339–1342.

Hoefen, T.M., Clark, R.N., Bandfield, J.L., Smith, M.D. Pearl, J.C., and Christensen, P.R. (2003) Discovery of olivine in the Nili Fossae region of Mars. *Science*, **302**, 627–630.

Hower, J., Eslinger, E.V., Hower, M.E., and Perry, E.A. (1976) Mechanism of burial metamorphism of argillaceous sediments: 1. Mineralogical and chemical evidence. *Geological Society of America Bulletin*, **87**, 725–737.

Hunt, G.R. and Salisbury, J.W. (1970) Visible and near-infrared spectra of minerals and rocks: I silicate minerals. *Modern Geology*, **1**, 283–300.

Jakosky, B.M. and Jones, J.H. (1994) Evolution of water on Mars. *Nature*, **370**, 328–329.

King, T.V.V. and Clark, R.N. (1989) Spectral characteristics of chlorites and Mg-serpentines using high resolution reflectance spectroscopy. *Journal of Geophysical Research*, **94**(B10), 13,997–14,008.

Kozak, P.K., Duke, E.F., and Roselle, G.T. (2004) Mineral distribution in contact-metamorphosed siliceous dolomite at Ubehebe Peak, California, based on airborne imaging spectrometer data. *American Mineralogist*, **89**, 5–6, 701–703.

Kruse, F.A. and Hauff, P.L. (1991) Identification of illite polytype zoning in disseminated gold deposits using reflectance spectroscopy and X-ray diffraction – Potential for mapping with imaging spectrometers. *IEEE Transactions on Geoscience and Remote Sensing (TGARS)*, **29**(1), 101–104.

Malin, M.C., Bell, J., Cantor, B., Caplinger, M., Calvin, W., Clancy, T., Edgett, K., Edwards, L., Haberle, R., James, P., Lee, S., Ravine, M., Thomas, P., and Wolff, M. (2007) Context Camera Investigation on board the Mars Reconnaissance Orbiter. *Journal of Geophysical Research*, **112**, E05S04, doi: 10.1029/2006JE002808.

McEwen, A.S., Eliason, E., Bergstrom, J., Bridges, N., Hansen, C., Delamere, W., Grant, J., Gulick, V., Herkenhoff, K., Keszthelyi, L., Kirk, R., Mellon, M., Squyres, S., Thomas, N., and Weitz, C. (2007), Mars Reconnaissance Orbiter's High Resolution Imaging Science Experiment (HiRISE). *Journal of Geophysical Research*, **112**, E05S02, doi: 10.1029/2005JE002605.

McLennan, S.M. (2003) Sedimentary silica on Mars. *Geology*, **31**, 315–318.

McSween, H.Y. Taylor, G.J., and Wyatt, M.B. (2009) Elemental composition of the Martian crust. *Science*, **324**, 736–739.

Melosh, H.J. (1989) *Impact Cratering: a Geologic Process.* Oxford University Press, Oxford, UK, 245 pp.

Merriman, R.J. and Peacor, D.R. (1999) Very low-grade metapelite: mineralogy, microfabrics and measuring reaction progress. Pp. 10–60 in: *Low-grade Metamorphism* (M. Frey and D. Robinson, editors). Blackwell, Oxford, UK.

Meunier, A. (2005) *Clays*. Springer, Berlin, 472 pp.

Milliken, R.E., Swayze, G., Arvidson, R., Bishop, J., Clark, R., Ehlmann, B., Green, R., Grotzinger, J., Morris, R., Murchie, S., Mustard, J., and Weitz, C. (2008) Opaline silica in young deposits on Mars. *Geology*, **36**, 847– 850, doi: 10.1130/G24967A.1.

Milliken, R.E., Bish, D.L., Bristow, T., and Mustard, J.F. (2010) The case for mixed-layered clays on Mars. *Lunar and Planetary Science Conference*, 41, abstract 2030.

Mumma, M., Villanueva, G., Novak, R., Hewagama, T., Bonev, B., DiSanti, M., Mandell, A., and Smith, M. (2009) Strong release of methane on Mars in Northern Summer 2003. *Science*, **323**, 1041–1045.

Murchie, S.L., Arvidson, R., Bedini, P., Beisser, K., Bibring, J.-P., Bishop, J., Boldt, J., Cavender, P., Choo, T., Clancy, R., Darlington, E., Des Marais, D., Espiritu, R., Fort, D., Green, R., Guinness, E., Hayes, J., Hash, C., Heffernan, K, Hemmler, J., Heyler, G., Humm, D., Hutcheson, J., Izenberg, N., Lee, R., Lees, J., Lohr, D., Malaret, E., Martin, T., McGovern, J., McGuire, P., Morris, R., Mustard, J., Pelkey, S., Rhodes, E., Robinson, M., Roush, T., Schaefer, E., Seagrave, G., Seelos, F., Silvergate, P., Slavney, S., Smith, M., Shyong, W.-J., Strohbehn, K., Taylor, H., Thompson, P., Tossman, B., Wirzburger, M., and Wolff, M. (2007) Compact Reconnaissance Imaging Spectrometer for Mars (CRISM) on Mars Reconnaissance Orbiter (MRO). *Journal of Geophysical Research*, **112**, E05S03, doi: 10.1029/2006JE002682.

Murchie, S.L., Mustard, J., Ehlmann, B., Milliken, R., Bishop, J., McKeown, N., Noe Dobrea, E., Seelos, F., Buczkowski, D., Wiseman, S., Arvidson, R., Wray, J., Swayze, G., Clark, R., Des Marais, D., McEwen, A., and Bibring, J.-P. (2009a) A synthesis of Martian aqueous mineralogy after one Mars year of observations from the Mars Reconnaissance Orbiter. *Journal of Geophysical Research*, **114**, E00D06, doi: 10.1029/2009JE003342.

Murchie, S.L., Seelos, F., Hash, C., Humm, D., Malaret, E., McGovern, A., Choo, T., Seelos, K., Buczkowski, D., Morgan, M., Barnouin-Jha, O., Nair, H., Taylor, H., Patterson, G., Harvel, C., Mustard, J., Arvidson, R., McGuire, P., Smith, M., Wolff, M., Titus, T., Bibring, J.-P., and Poulet, F. (2009b) The CRISM investigation and data set from the Mars Reconnaissance Orbiter's Primary Science Phase. *Journal of Geophysical Research*, **114**, E00D07, doi: 10.1029/2009JE003344.

Mustard, J.F., Poulet, F., Head, J., Mangold, N., Bibring, J.-P., Pelkey, S., Fassett, C., Ngevin, Y., and Neukum, G. (2007) Mineralogy of the Nili Fossae region with OMEGA/Mars Express data: 1. Ancient impact melt in the Isidis Basin and implications for the transition from the Noachian to Hesperian. *Journal of Geophysical Research*, **112**, E08S03, doi: 10.1029/2006JE002834.

Mustard, J.F., Murchie, S., Pelkey, S., Ehlmann, B., Milliken, R., Grant, J., Bibring, J.-P., Poulet, F., Bishop, J., Noe Dobrea, E., Roach, L., Seelos, F., Arvidson, R., Wiseman, S., Green, R., Hash, C., Humm, D., Malaret, E., McGovern, J., Seelos, K., Clancy, T., Clark, R., Des Marais, D., Izenberg, N., Knudson, A., Langevin, Y., Martin, T., McGuire, P., Morris, R., Robinson, M., Roush, T., Smith, M., Swayze, G., Taylor, H., Titus, T., and Wolff, M. (2008) Hydrated silicate minerals on Mars observed by the CRISM instrument on MRO. *Nature*, **454**, 305– 309, doi: 10.1038/nature07097.

Mustard, J.F., Ehlmann, B., Murchie, S., Poulet, F., Mangold, N., Head, J., Bibring, J.-P., and Roach, L. (2009) Composition, morphology, and stratigraphy of Noachian crust around the Isidis basin. *Journal of Geophysical Research*, **114**, E00D12, doi: 10.1029/2009JE003349.

Newsom, H.E. (1980) Hydrothermal alteration on impact melt sheets with implications for Mars: *Icarus*, **44**, 207–216, doi: 10.1016/0019-1035(80)90066-4.

Parente, M. (2008) A new approach to denoising CRISM images. *Lunar Planetary Science Conference*, **39**, abstract #2528.

Parmentier, E.M. and Zuber, M.T. (2007) Early evolution of Mars with mantle compositional stratificationn or hydrothermal crustal cooling. *Journal of Geophysical Research*, **112**, E05014, doi: 10.1029/2006JE002734.

Pelkey, S.M., Mustard, J., Murchie, S., Clancy, R., Wolff, M., Smith, M., Milliken, R., Bibring, J.-P., Gendrin, A., Poulet, F., Langevin, Y., and Gondet, B. (2007) CRISM multispectral summary products: Parameterizing mineral diversity on Mars from reflectance. *Journal of Geophysical Research*, **112**, E08S14, doi: 10.1029/2006JE002831.

Philpotts, A.R. and Ague, J.J. (2009) *Principles of Igneous and Metamorphic Petrology*, 2nd edition. Cambridge University Press, New York, 667 pp.

Poulet, F., Bibring, J.-P., Mustard, J., Gendrin, A., Mangold, N., Langevin, Y., Arvidson, R., Gondet, B., Gomez, C., and the OMEGA team (2005) Phyllosilicates on Mars and implications for early Martian climate. *Nature*, **438**, 623–627, doi: 10.1038/nature04274.

Rathbun, J.A. and Squyres, S.W. (2002) Hydrothermal systems associated with Martian Impact Craters. *Icarus*, **157**, 362–372.

Robinson, D. and Bevins, R.E. (1999) Patterns of regional low-grade metamorphism in metabasites. Pp. 143–168 in: *Low-grade Metamorphism* (M. Frey and D. Robinson, editors). Blackwell, Oxford, UK.

Rogers, A.D. and Christensen, P.R. (2007) Surface mineralogy of Martian low-albedo regions from MGS-TES data: Implications for upper crustal evolution and surface alteration. *Journal of Geophysical Research*, **112**, E01003, doi:

10.1029/2006JE002727.
Rosenberg, P.E. (2002) The nature, formation, and stability of end-member illite: A hypothesis. *American Mineralogist*, **87**, 103–107.
Ruff, S.W. (2004) Spectral evidence for zeolite in the dust on Mars. *Icarus*, **168**, 131–143. doi: 10.1016/j.icarus.2003.11.003.
Schiffman, P. and Day, H.W. (1999) Petrological methods for the study of very low grade metabasites. Pp. 108–142 in: *Low-grade Metamorphism* (M. Frey and D. Robinson, editors). Blackwell, Oxford, UK.
Schwenzer, S.P. and Kring, D.A. (2009) Impact-generated hydrothermal systems capable of forming phyllosilicates on Noachian Mars. *Geology*, **37**, 1091–1094.
Skok, J.R., Mustard, J.F., Ehlmann, B.L., Milliken, R.E., and Murchie, S.L. (2010) Silica deposits in the Nili Patera caldera on the Syrtis Major volcanic complex on Mars. *Nature Geoscience*, doi: 10.1038/ngeo990.
Smulikowski, W., Desmons, J., Harte, B., Sassi, F.P., and Schmid, R. (2003) A systematic nomenclature for metamorphic rocks: 2. Types, grade and facies of metamorphism. *Recommendations by the IUGS Subcommission on the Systematics of Metamorphic Rocks*. SCMR website (www.bgs.ac.uk/SCMRH).
Spear, F.S. (1995) *Metamorphic Phase Equilibria and Pressure-Temperature-Time Paths.* Mineralogical Society of America Monograph, Washington, D.C., 799 pp.
Środoń, J. (1999) Nature of mixed-layer clays and mechanisms of their formation and alteration. *Annual Review of Earth and Planetary Science*, **27**, 19–53.
Swayze, G.A., Milliken, R., Clark, R., Bishop, J., Ehlmann, B., Pelkey, S., Mustard, J., and Murchie, S. (2007) Spectral evidence for hydrated volcanic and/or impact glass on Mars with MRO CRISM. *Seventh International Conference on Mars*, abstract 1353.
Swayze, G.A., Kokaly, R.F., Higgins, C.T., Clinkenbeard, J.P., Clark, R.N., Lowers, H.A., and Sutley, S.J. (2009) Mapping potentially asbestos-bearing rocks using imaging spectroscopy. *Geology*, **37**, 763–766.
Tosca, N.J. and Knoll, A.H. (2009) Juvenile chemical sediments and the long term persistence of water at the surface of Mars. *Earth and Planetary Science Letters*, **286**, 379–386.
Velde, B. and Iijima, A. (1988) Comparison of clay and zeolite mineral occurrences in Neogene age sediments from several deep wells. *Clays and Clay Minerals*, **36**, 337–342.
Whitney, G. (1990) Role of water in the smectite-to-illite reaction. *Clays and Clay Minerals*, **38**, 343–350.
Wiesenberger, T. and Selbekk, R.S. (2008) Multi-stage zeolite facies mineralization in the Hvalfjordur area, Iceland. *International Journal of Earth Sciences*, doi: 10.1007/s00531-007-0296-6.
Yau, Y.-C., Peacor, D.R., Beane, R.E., Essene, E.J., and McDowell, S.D. (1988) Microstructures, formation mechanisms, and depth-zoning of phyllosilicates in geothermally altered shales, Salton Sea, California. *Clays and Clay Minerals*, **36**, 1–10.
Zwart, H.J., Corvalon, J., James, H.L., Miyashira, A., Saggerson, E.P., Sobolev, V.S., Subramaniam, A.P., and Vallance, T.G. (1967) A scheme of metamorphic facies for cartographic representation. International Union of Geological Sciences. *Geological Newsletter*, **2**, 57–74.

(*Received 31 March 2010; revised 11 August 2011; Ms. 424; A.E. M. Velbel*)